Special Report on the
Zeerijp Earthquake – 8th January 2018

Datum	January 2018
Editors	Taco den Bezemer and Jan van Elk

Contents

1 Summary

This Special Report, which was announced in NAM's letter of 10th January 2018 (NAM, 2018a), has been prepared, in accordance with the Measurement and Control protocol (MRP) (NAM, 2017a). It addresses the earthquake on the 8th January 2018 at 3 pm, near the village of Zeerijp. The Zeerijp earthquake had a magnitude of 3.4 on the Richter Scale, as established by KNMI. The earthquake was widely felt and caused (DS1) damage to buildings. No falling objects (e.g. chimneys) or injuries have been reported.

In this report, the measurements and observations obtained during the Zeerijp earthquake are analysed in chapter 3. The assessment of these measurements and observations of ground motions and building damage showed that in all aspects, the Zeerijp earthquake was within the anticipated range indicated by modelling for the Hazard and Risk Assessment. No special characteristics of the Zeerijp earthquake, deviating from the modelling, have been identified. On this basis, no revision of the Hazard and Risk Assessment is required at this time.

In chapter 4, the report provides an overview of the status and trend of all parameters used in the MRP framework. This showed the intervention level in the MRP has been reached for PGA and the intervention level on earthquake density is being approached. Based on this analysis and line with the MRP, NAM has advised potential measures in its letter to the Minister of 10th January 2018. The expected effects on seismicity and the parameters in the MRP are discussed in chapter 5.

The analyses described above, which have been more extensive than those prepared in the first 48 hours after the earthquake, do not lead to a requirement to revise and restate NAM's assessment of the situation, as described in its letters to SodM of 10th and 17th January 2018.

2 Introduction

This Special Report has been prepared, in accordance with the Measurement and Control protocol (MRP) (NAM, 2017a), following the earthquake on the 8th January 2018 at 3 pm, near the village of Zeerijp. This was the third largest earthquake in Groningen, following the Westeremden earthquake of 8th August 2006, with a magnitude of 3.5, and the Huizinge earthquake of 16th August 2012, with a magnitude of 3.6 on the Richter Scale.

During this earthquake, one of the KNMI stations, registered a ground acceleration in excess of 0.1 g. As a result, the intervention level threshold of the Measurement and Control Protocol (MRP) was exceeded. In line with the response processes described in the Measurement and Control Protocol the Risk Coordination Team (RCT)[1] of NAM met that same day and again the following day to analyse the event and discuss control measures.

The Zeerijp earthquake had a magnitude of 3.4 on the Richter Scale, as established by KNMI. The earthquake was widely felt and caused (DS1) damage to many buildings. Using the methodology developed by USGS, "Did you feel it?" (USGS, 2011), the earthquake was felt at a large distance from the epicentre, including parts of the city of Groningen. Some 65,000 houses[2] are located in the area, where the earthquake was felt. Especially in the area near Zeerijp, where the largest vertical accelerations have been recorded, the earthquake has been experienced as frightening.

The number of buildings that have been exposed to a probability of more than 0.1% of aesthetic damage (DS1) is currently estimated at some 18,000 houses (an area of approximately 10 km around the earthquake epicentre). Some 1,000 buildings are located in the area where the probability of damage is larger than 10% (within a 3 km distance from the epicentre). In the 10 days following the earthquake (from 8th January to 18th January 2018) some 3,749 building damage cases were reported to the Centrum Veilig Wonen (CVW).

After preliminary analysis of the available data, a letter (NAM, 2018a) was prepared detailing the initial assessment of the impact of the earthquake and providing the Minister of Economic Affairs and Climate with potential control measures for his consideration. This letter was shared with SodM within 48-hours of the Zeerijp earthquake and prepared in agreement with the requirements in the MRP.

This letter was followed by an additional letter (NAM, 2018b), providing further clarification on the expected effects of potential control measures. The current "Special Report on the Zeerijp Earthquake – 8th January 2018" presents the technical analysis carried out during the 10-day period following the Zeerijp earthquake. In detail, some of the technical conclusions have been further refined since these letters were prepared, although no fundamental new insights have come to light since then. As studies continue new insights might develop.

---

[1] The MPR prescribes the RCT needs to meet within 24 hours.
2 In the "48-hour letter" sent to SodM within 48 hours of the Zeerijp earthquake (10th January 2018), it was erroneously reported that some 65,000 people lived in the area where the earthquake was felt.

3 Analysis of Measurements and Observations of the Zeerijp Earthquake

In this section of the Special Report the measurements and observations of the Zeerijp Earthquake are reported and discussed. An initial analysis of these measurements and observations is provided, focussing on the assurance of the hazard and risk modelling.

3.1 Surface Ground Motions measured by KNMI Network

3.1.1 Introduction

On Monday 8th January 2018 at 14:00:52 UTC (3 pm local time), an earthquake occurred near the village of Zeerijp in the municipality of Loppersum (Figure 1). In common with all induced earthquakes in the Groningen field, a focal depth of 3 km was assigned by KNMI[3], who reported a local magnitude of M_L 3.4. This is the third largest earthquake to have occurred in the Groningen field, the largest being the M_L 3.6 Huizinge earthquake of August 2012 and the second largest the M_L 3.5 Westeremden earthquake of August 2006.
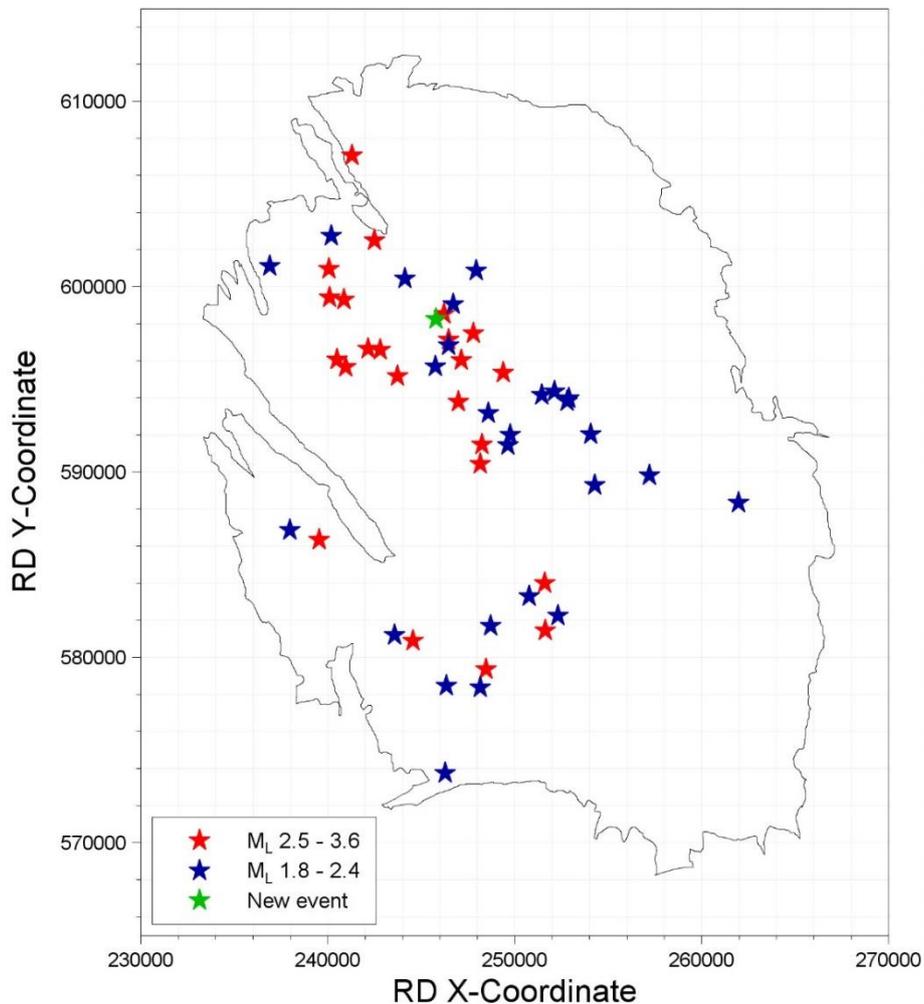
*Figure 1   Epicentre of Zeerijp earthquake (green star) together with epicentres of previous earthquakes of $M_L \geq 2.5$ (red stars) and of M_L 1.8 - 2.4 (blue stars).*

---

3 In section 3.2 of this report the determination of the hypocentre of the Zeerijp earthquake is discussed. With the Full Waveform Inversion (FWI) the hypocentre is determined to fall within the reservoir, located at some 3 km.

In line with the trend of recent earthquakes such as the M_L 3.1 Hellum earthquake of September 2015 and the M_L 2.6 Slochteren earthquake of May 2017 (Figure 2), the latest earthquake has triggered a large number of accelerograms, as a direct result of the expansion of the strong-motion recording networks in the Groningen field (Dost *et al.*, 2018). The Slochteren earthquake, despite its modest magnitude, contributed 68 new recordings to the Groningen ground motion database.
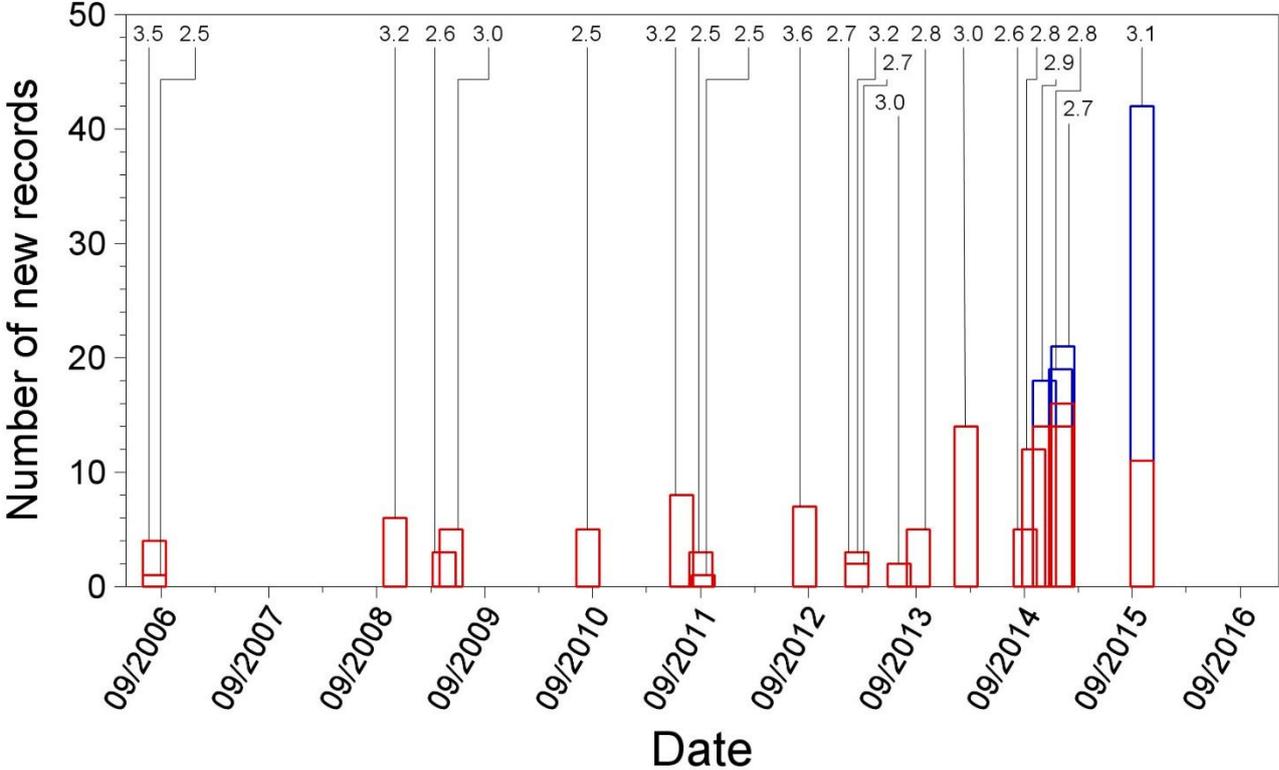

Figure 2   Diagram illustrating the timing of earthquakes of $M_L \geq 2.5$ in the Groningen field and the number of records yielded by the permanent KNMI network (B-stations, red) and by the expanded borehole geophone network (G-stations, blue). The 2017 Slochteren earthquake added an additional 68 records to the database. Figure from Bommer et al. (2018).

The KNMI portal (http://rdsa.knmi.nl/opencms/nl-rrsm) made accelerograms from the earthquake available within an hour of the event and 79 three-component recordings were downloaded and processed for this preliminary assessment of the motions. Figure 3 shows these recordings as contained in the database used to derive the current ground motion model used for seismic hazard and risk analyses in the Groningen field. This report presents an overview of the recorded motions in terms of their amplitudes and durations, and discusses how the recorded amplitudes of motion compare with predictions from the ground motion models. The discussions focus primarily on peak ground acceleration (PGA), which is assumed equal to the spectral acceleration at a period of 0.01 seconds, and peak ground velocity (PGV), which has been shown to correlate very well with the spectral acceleration at a period of 0.3 seconds for the Groningen data (Figure 4).
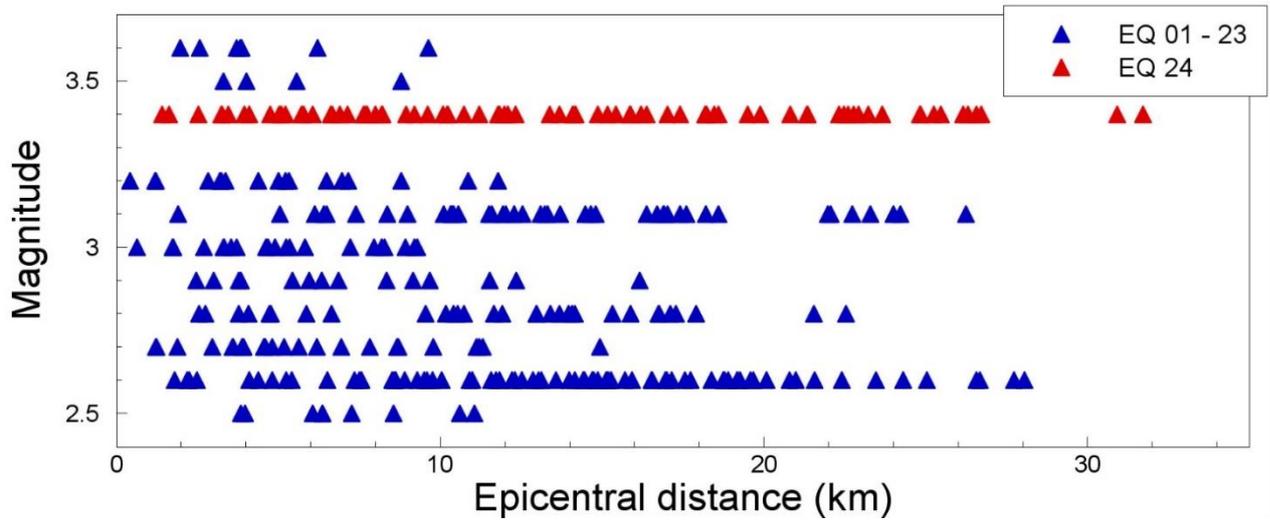
Figure 3   Magnitude-distance distribution of the Groningen strong-motion database including the recordings of the 2018 Zeerijp earthquake. The 79 recordings of the Zeerijp earthquake are shown in red. Above these recording are shown the 4 recordings of the Westeremden earthquake of 2006 and the 7 recordings of the Huizinge earthquake of 2012.
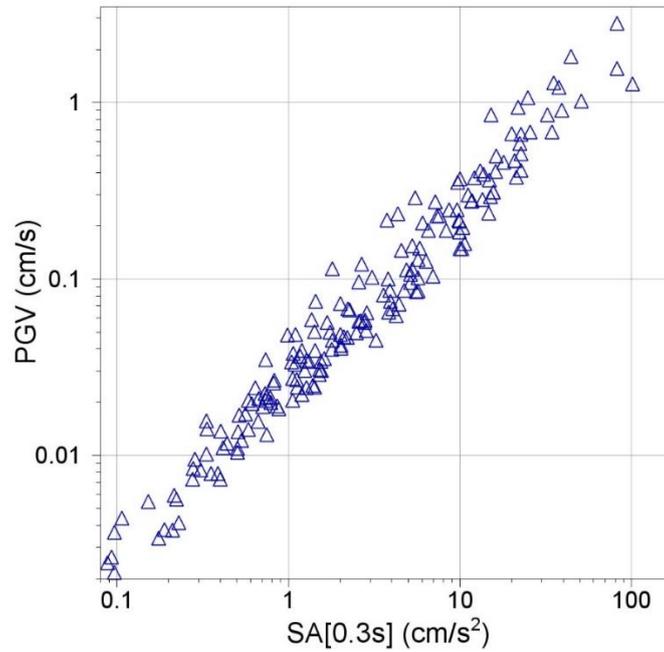
Figure 4   Correlation between values of PGV and spectral accelerations at 0.3 seconds for the Groningen strong-motion database (Bommer et al., 2018)

3.1.2 Peak Ground Accelerations and Velocities

Figure 5 shows the larger horizontal values of PGA and PGV from each recording obtained during the Zeerijp earthquake plotted against the distance of the recording site from the epicentre. The largest amplitudes were obtained at the BGAR station located 2.5 km from the epicentre: the PGAs recorded at this station are 108.4 cm/s^2 on the EW component and 71.0 cm/s^2 on the NS component. The largest PGV values are at the same station are 3.19 cm/s (EW) and 1.98 cm/s (NS). The EW component of the BGAR station is the only record to exceed to previous maximum PGA value recorded during the Huizinge earthquake.
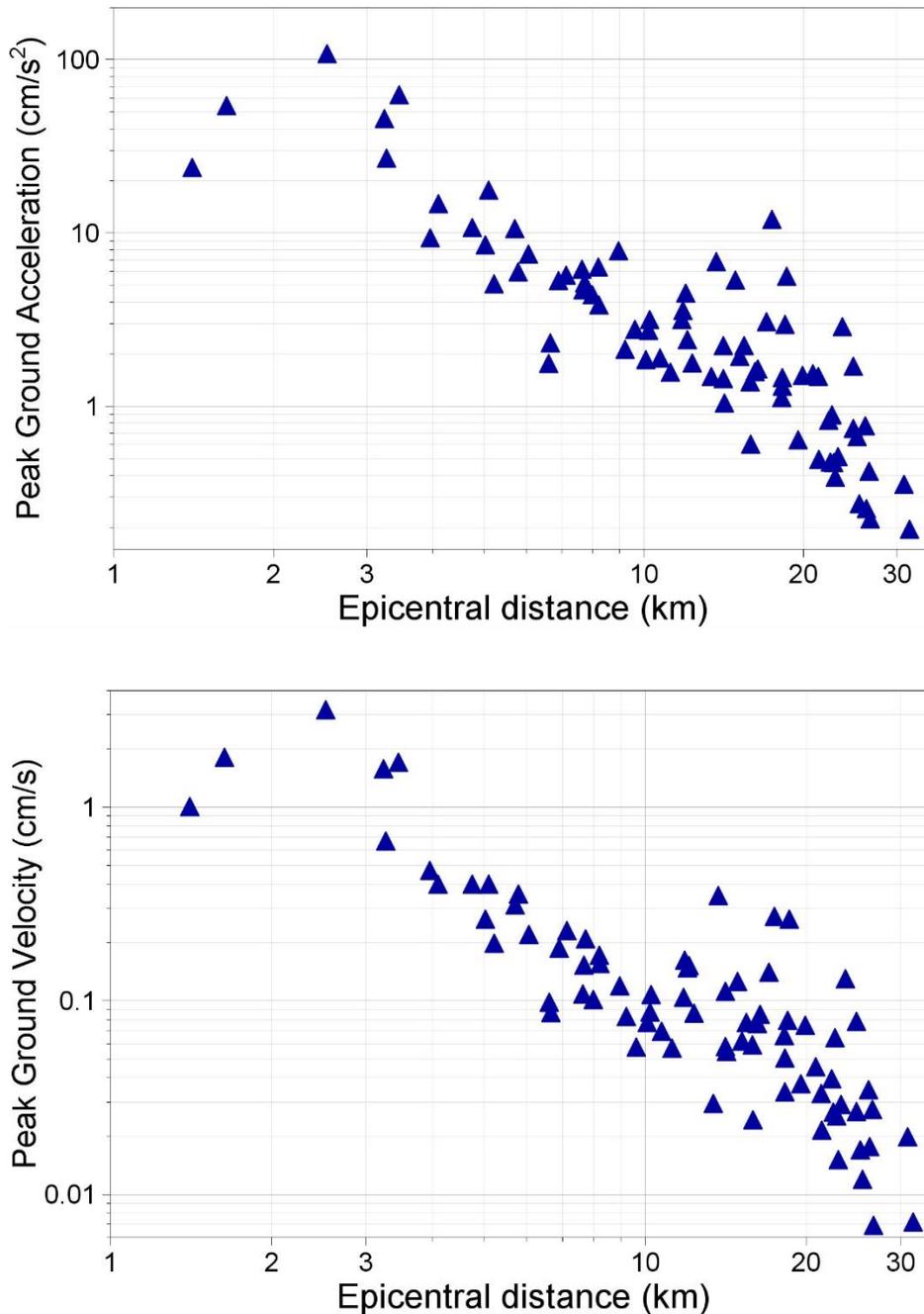
Figure 5   Larger as-recorded horizontal components of PGA (upper) and PGV (lower) recorded during the Zeerijp earthquake plotted against epicentral distance

A striking feature of Figure 5 are the lower amplitudes recorded closer to the epicentre at the BZN1 and G140 stations. The differences are unlikely to be explained by differences in site profiles since all

three stations have almost identical values of the time-averaged shear-wave velocity over the upper 30 metres (Kruiver *et al.*, 2017; Noorlandt *et al.*, 2018), which are all equal to 192 or 193 m/s. Figure 6 shows the horizontal components of PGA and PGV obtained within 5 km of the epicentre, from which it can be appreciated that the strong polarisation often observed in Groningen recordings (*e.g.*, Bommer *et al.*, 2017a) is not particularly marked for this event.
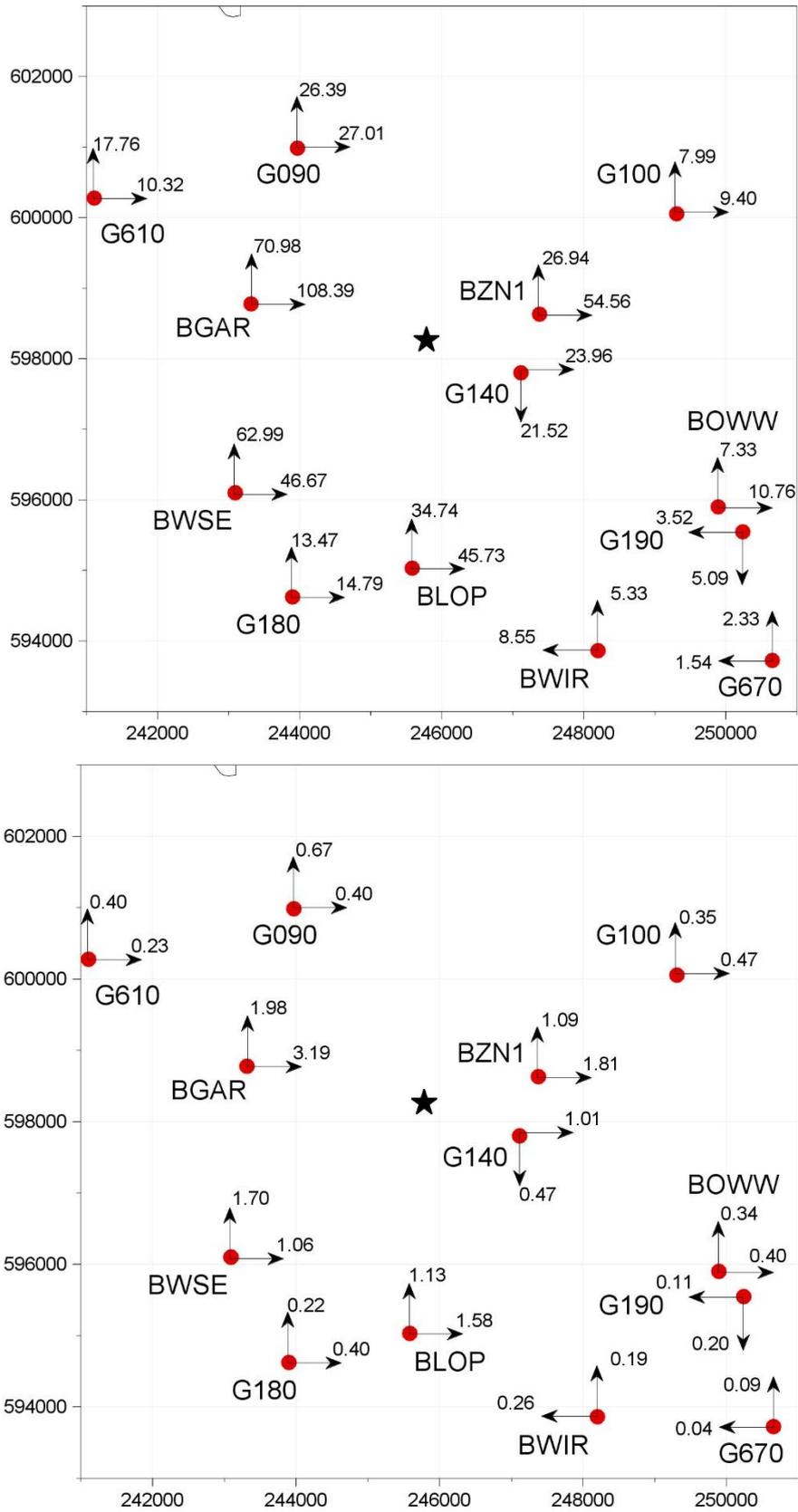
*Figure 6   Horizontal components of PGA (upper) and PGV (lower) recorded during the Zeerijp earthquake at epicentral distances of less than 5 km; units are cm/s² and cm/s, respectively.*

As already shown in Figure 3, the amplitudes decay rapidly with distance although the effect of simultaneous arrivals of direct and critically refracted/reflected waves leads to an increase in amplitudes at some locations between 12 and 20 km from the epicentre. However, these effects do not lead to significant absolute amplitudes at those distances and it is clear from Figure 7 and Figure 8 that outside of the epicentral area the motions are generally of very low amplitude: < 0.02g for PGA and < 0.3 cm/s for PGV.
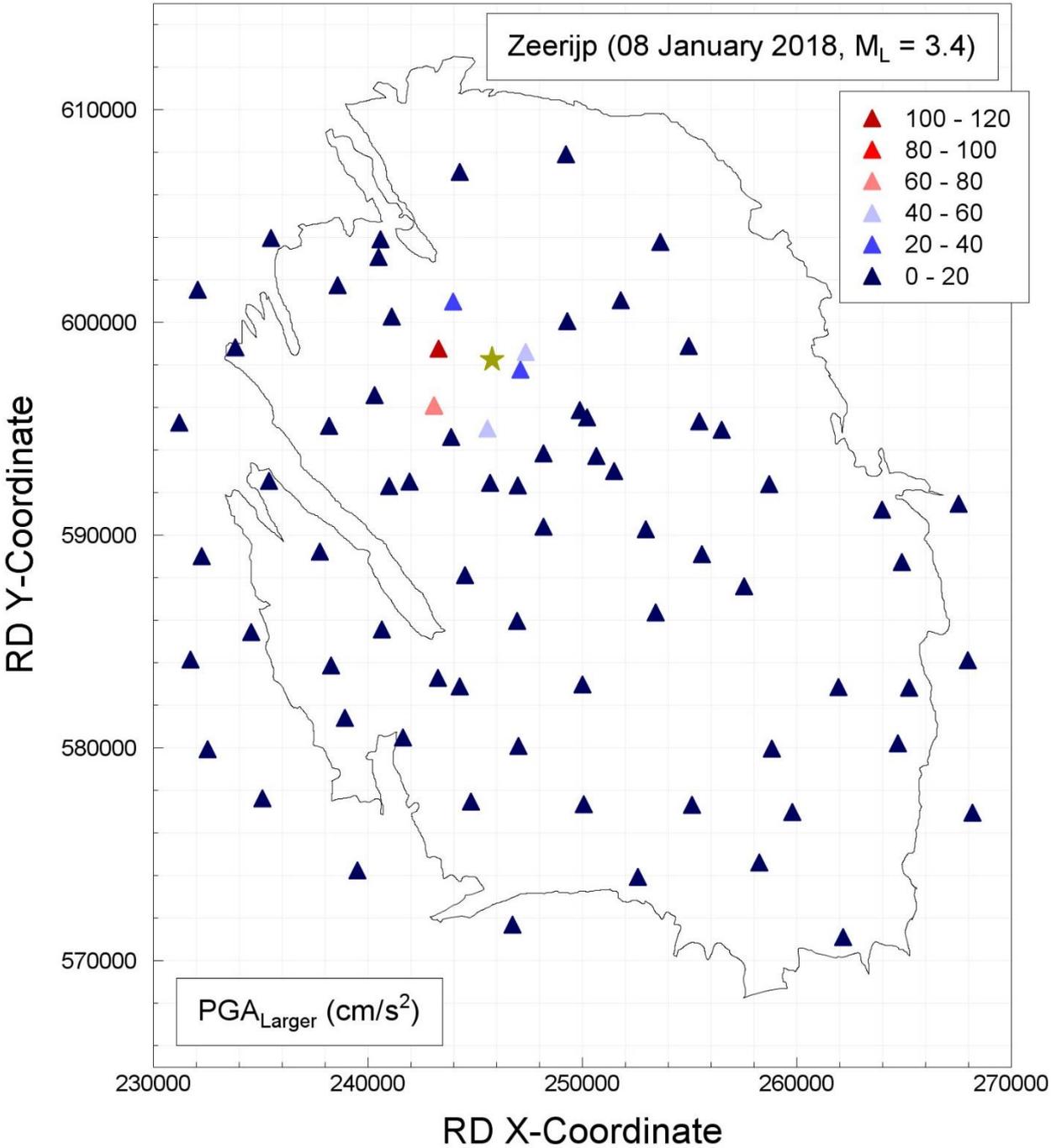
Figure 7   Map showing ranges of the larger component of PGA (cm/s^2) recorded at each station
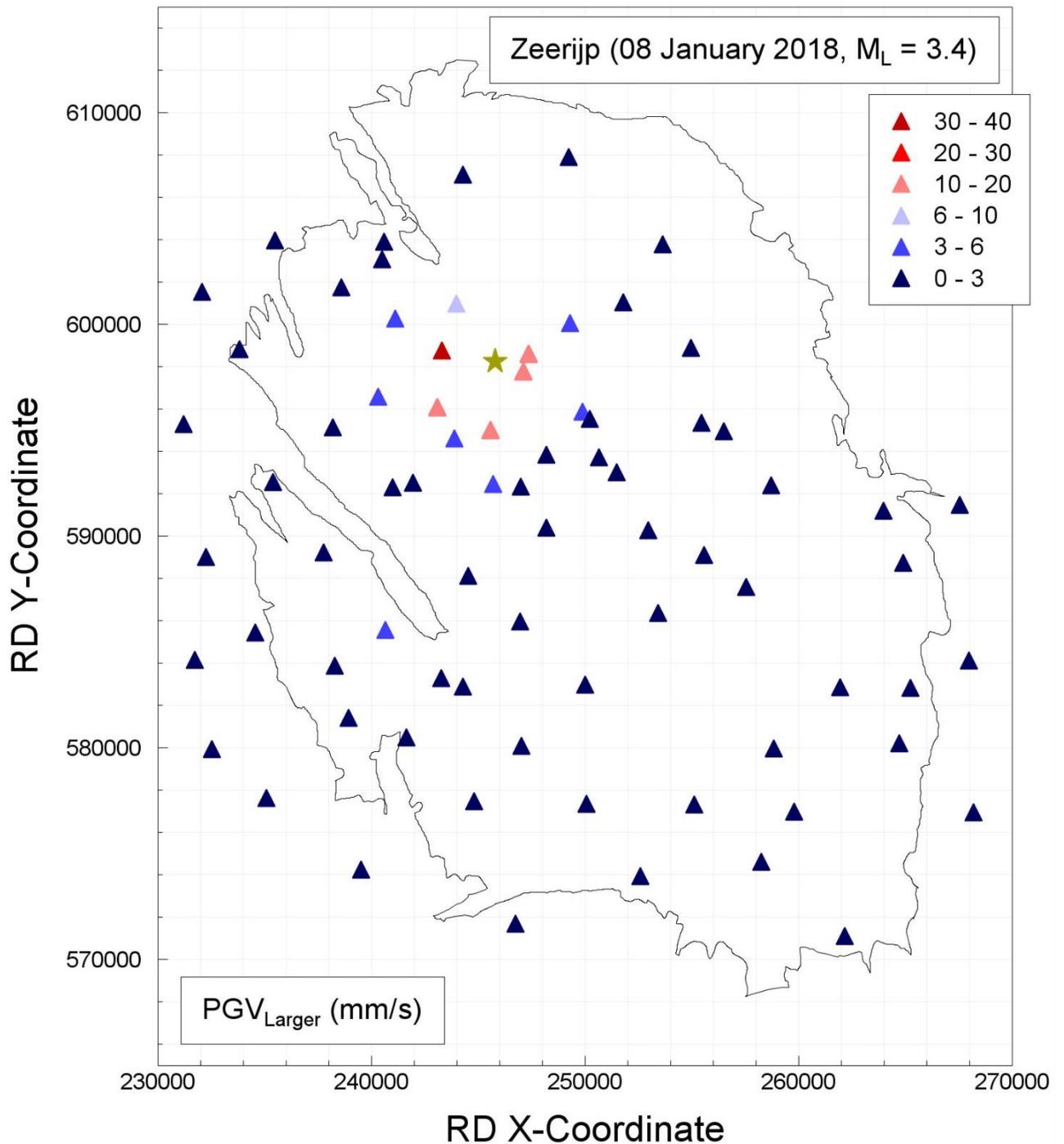
Figure 8   Map showing ranges of the larger component of PGV (note units: mm/s) recorded at each station

Overall, with the single exception of the EW component of the BGAR record, the motions are generally consistent with those observed in previous earthquakes. Figure 9 shows the geometric mean horizontal components of PGA and PGV plotted against magnitude together with the corresponding values from the complete database. The most striking feature is how this earthquake has contributed a large number of low-amplitude recordings, a feature also clearly visible for the M_L 2.6 Slochteren and M_L 3.1 Hellum earthquakes, reflecting the expansion of the recording networks in the Groningen field.
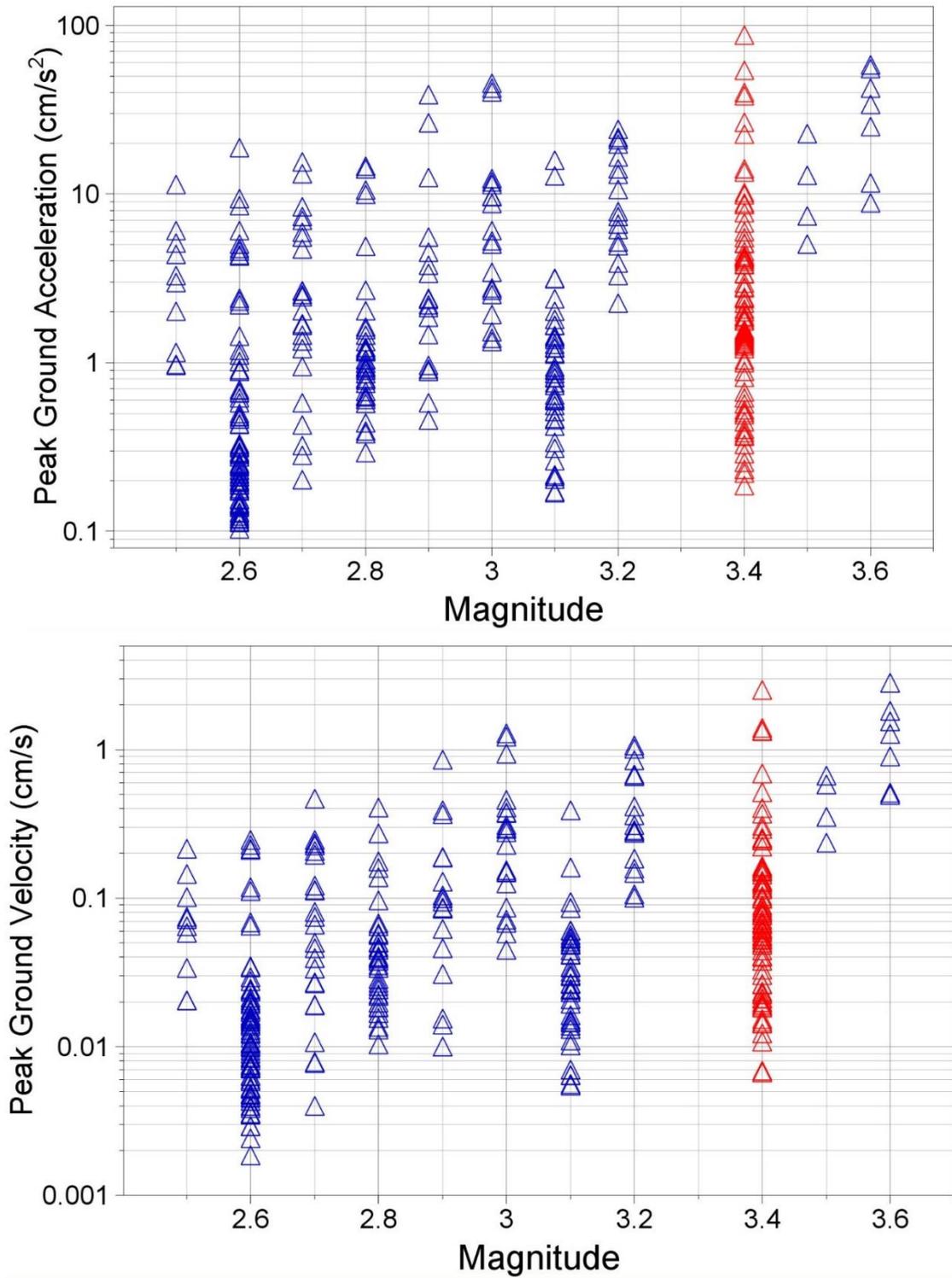
Figure 9   Geometric mean horizontal components of PGA (upper) and PGV (lower) recorded during the Zeerijp earthquake (red) and in previous earthquakes (blue) plotted against local magnitude

3.1.3 Ground Motion Durations

The maximum amplitude of ground shaking, whether represented by PGA or PGV, provides a simple indication of the strength of the motion but the potential for adverse effects—such as damage to masonry buildings or triggering liquefaction—also depends on the duration or number of cycles of the motion.

A feature that has been consistently observed in the Groningen ground motions is a very pronounced negative correlation between PGA and duration, with high amplitude motions consistently associated with shaking of very short duration (Bommer *et al.*, 2016). The same pattern is observed in the recordings of the Zeerijp earthquake, as shown in Figure 10. The largest value of PGA, recorded on the EW component at the BGAR station, is associated with a duration of less than half-a-second (0.43 s). The second highest PGA value is also from the BGAR station and is associated with a duration of just 0.54 s. The horizontal components of both acceleration and velocity from this station are shown in Figure 11, which also shows the build-up of Arias intensity (which is a measure of the energy in the motion) over time. The strong concentration of the energy in a single pulse of motion is immediately apparent. An equally pronounced case is seen for the BZN1 recording—the second closest instrument to the epicentre and source of the fourth largest value of PGA—where the larger amplitude component is associated with a significant duration of just 0.17 s (Figure 12).
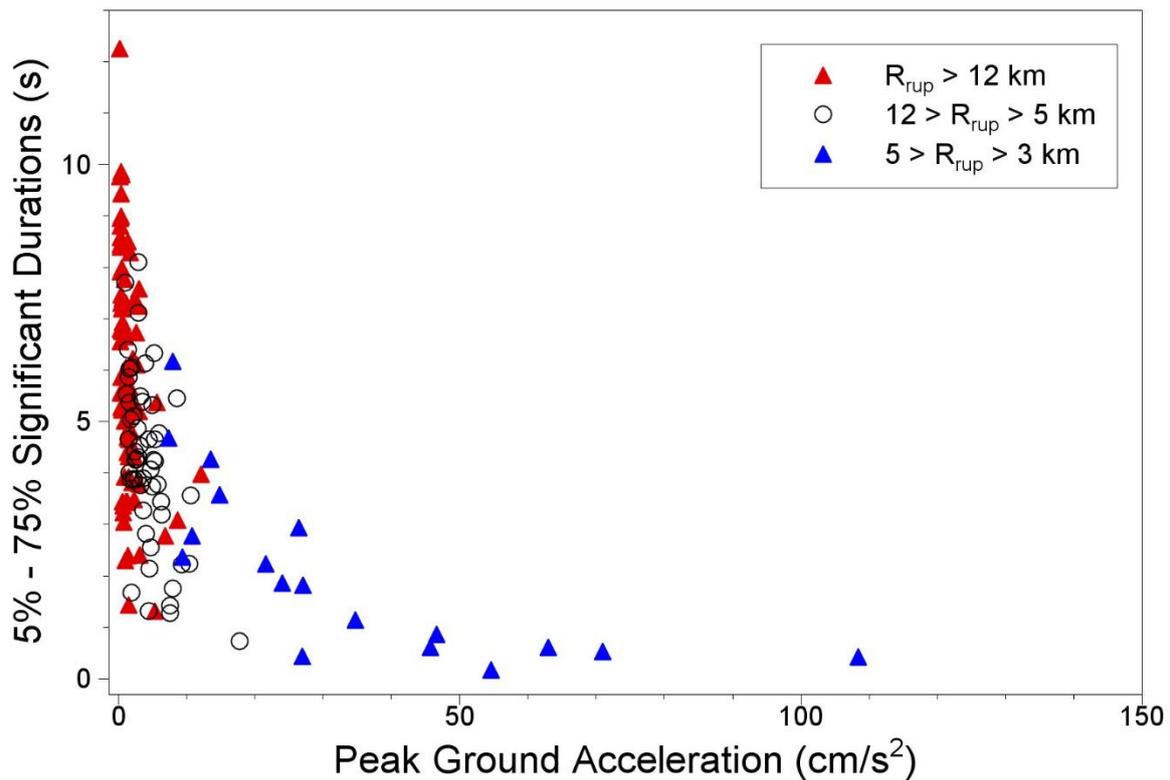
Figure 10   Pairs of PGA and significant duration for individual components of the Zeerijp records, with symbols indicating the rupture distance of the recording.
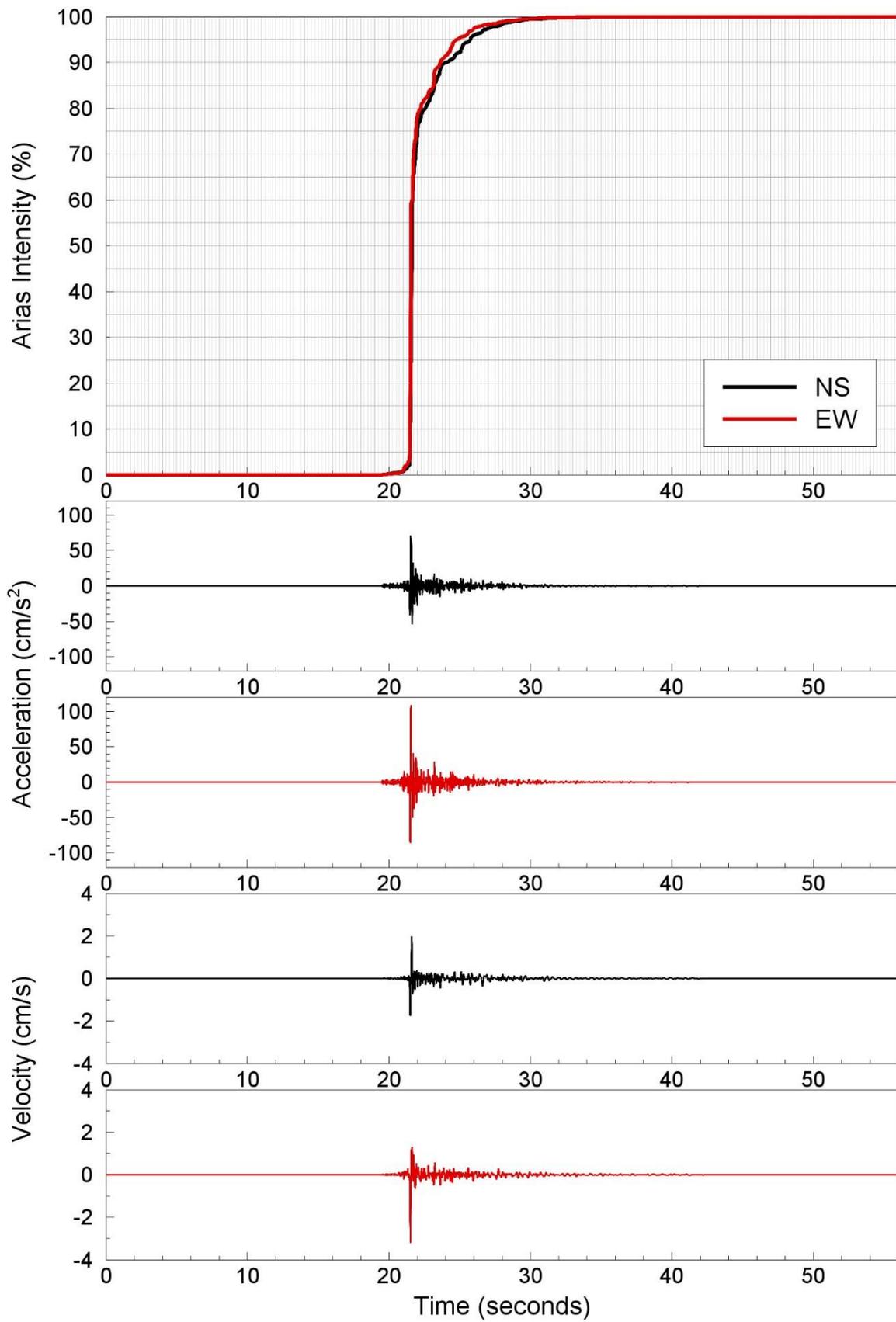
Figure 11   Horizontal components of acceleration and velocity from the BGAR station; the upper frame shows the accumulation of Arias intensity (energy) over time.
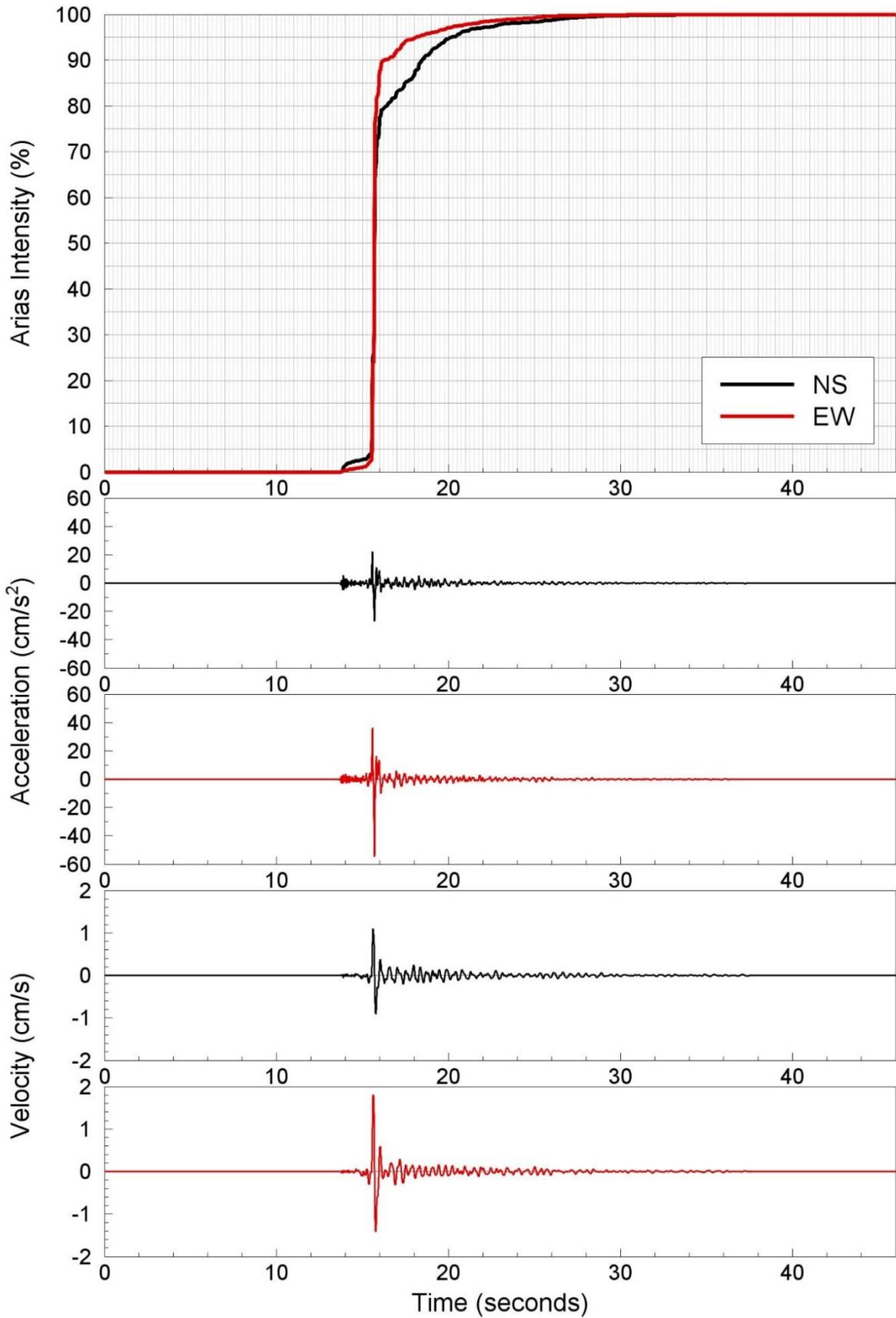
Figure 12 Horizontal components of acceleration and velocity from the BZN1 station; the upper frame shows the accumulation of Arias intensity (energy) over time.

3.1.4 Spectral Accelerations and Comparison with Ground Motion Models

The fragility functions used in the estimation of seismic risk in the Groningen field are defined in terms of response spectral accelerations at various oscillator periods (Crowley *et al.*, 2017). The horizontal acceleration response spectra from the BGAR recordings of the Zeerijp earthquake are shown in Figure 13. The peaks at about 0.07 and 0.15 seconds are consistent with the calculated linear amplification factors for this station, although it must be recognised that some non-linearity could have been caused by this earthquake at such close distance to the station (Bommer *et al.*, 2017b). The very different shapes of the spectra around 0.1 second, however, is likely to reflect source effects and the radiation pattern of seismic energy.
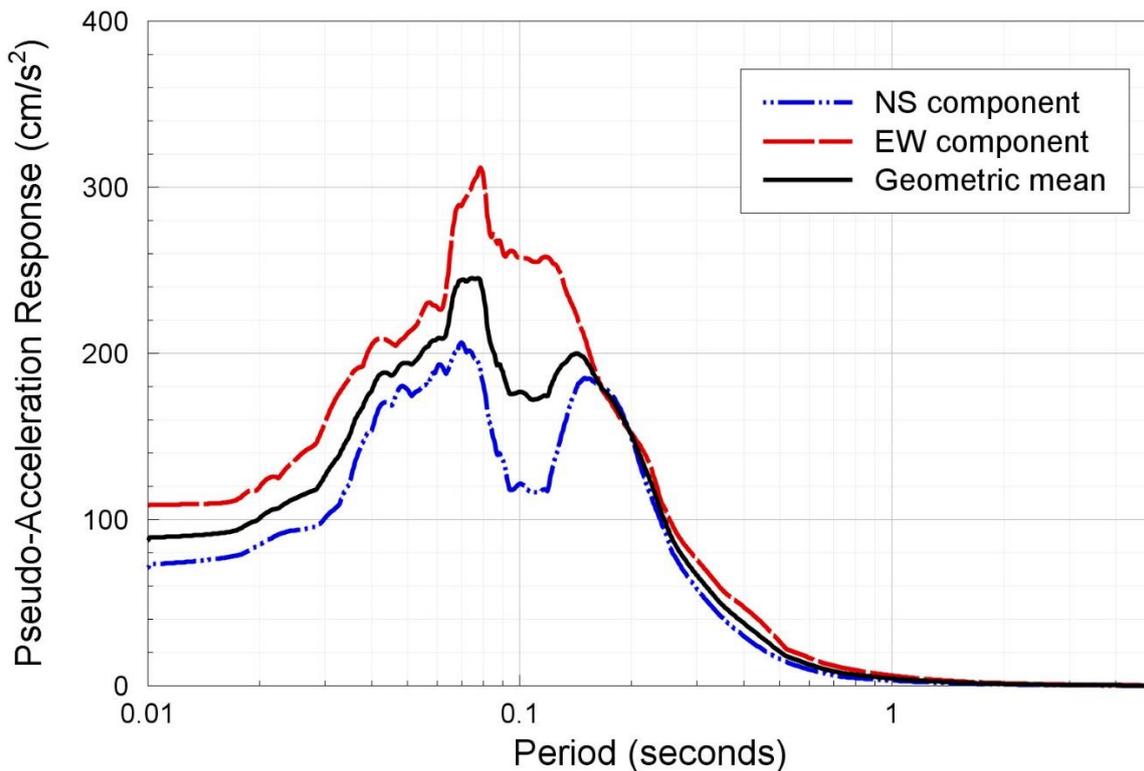

Figure 13   Horizontal response spectra from the BZN1 (upper) and BGAR (lower) stations

For this preliminary analysis, the key question of interest is whether the motions recorded in this earthquake are consistent with the current ground motion model (GMM) being used in the Groningen field. The current model is the V5 GMM developed last year (Bommer *et al.*, 2017b) and we have simply calculated the total residuals at the surface for different ground motion parameters. In each case, the residual is the natural logarithm of the ratio of the observed (recorded) to the median predicted value, so a residual of 0.7 indicates that the recorded value was underestimated by a factor of 2 by the model and a residual of -0.7 would indicate over-prediction by a factor of 2. Figure 14 shows the residuals of PGA and PGV with respect to the V5 GMM plotted against rupture distance. In both cases, the scatter is very considerable but it can also be observed that the PGA residuals are well centred about the zero line, which suggests that the model provides a reasonable overall fit to the data. For the PGV values, the residuals are slightly shifted towards negative values, which indicates that on average the model is over-predicting the level of peak ground velocity. The same patterns are observed for spectral accelerations, Sa, at other periods, with the residuals at short periods being generally centred (Figure 15) while at longer periods there is a consistent pattern of over-prediction by the V5 GMM (Figure 16).
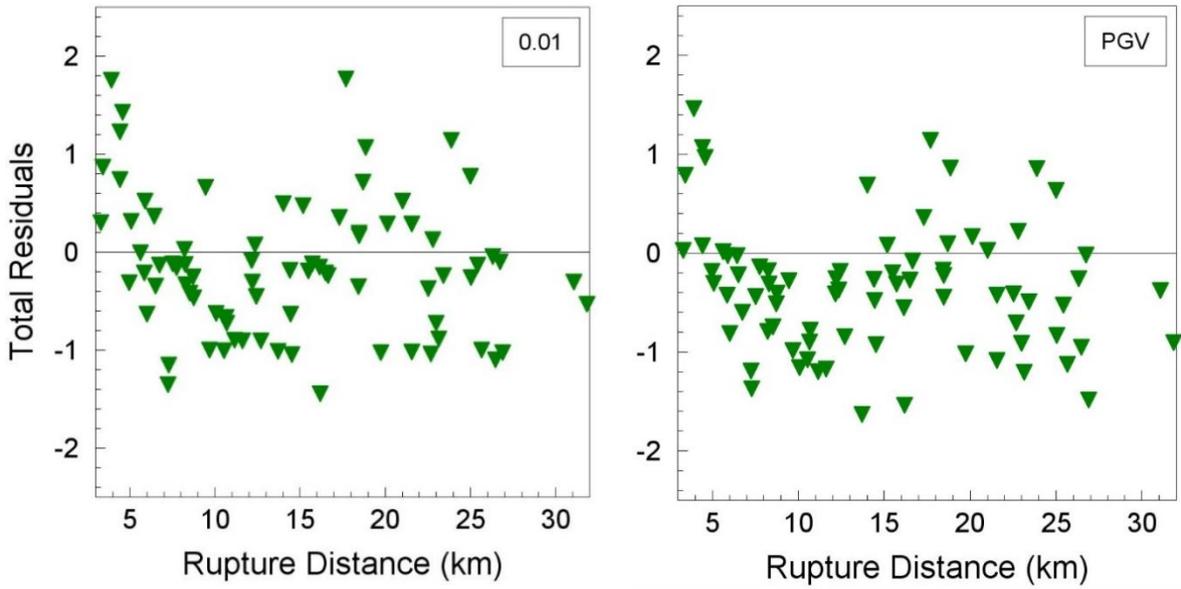
Figure 14   Residuals of PGA (left) and PGV (right) with respect to the central branch of the V5 GMM plotted against rupture distance.
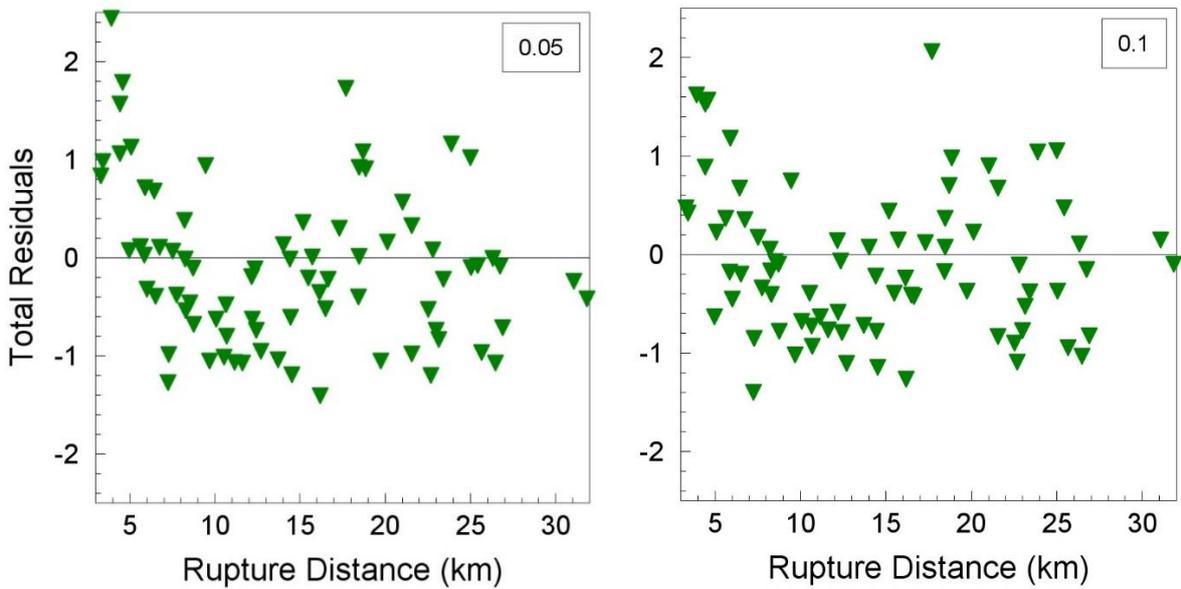
Figure 15   Residuals of Sa(0.05s) (left) and Sa(0.1s) (right) with respect to the central branch of the V5 GMM plotted against rupture distance.
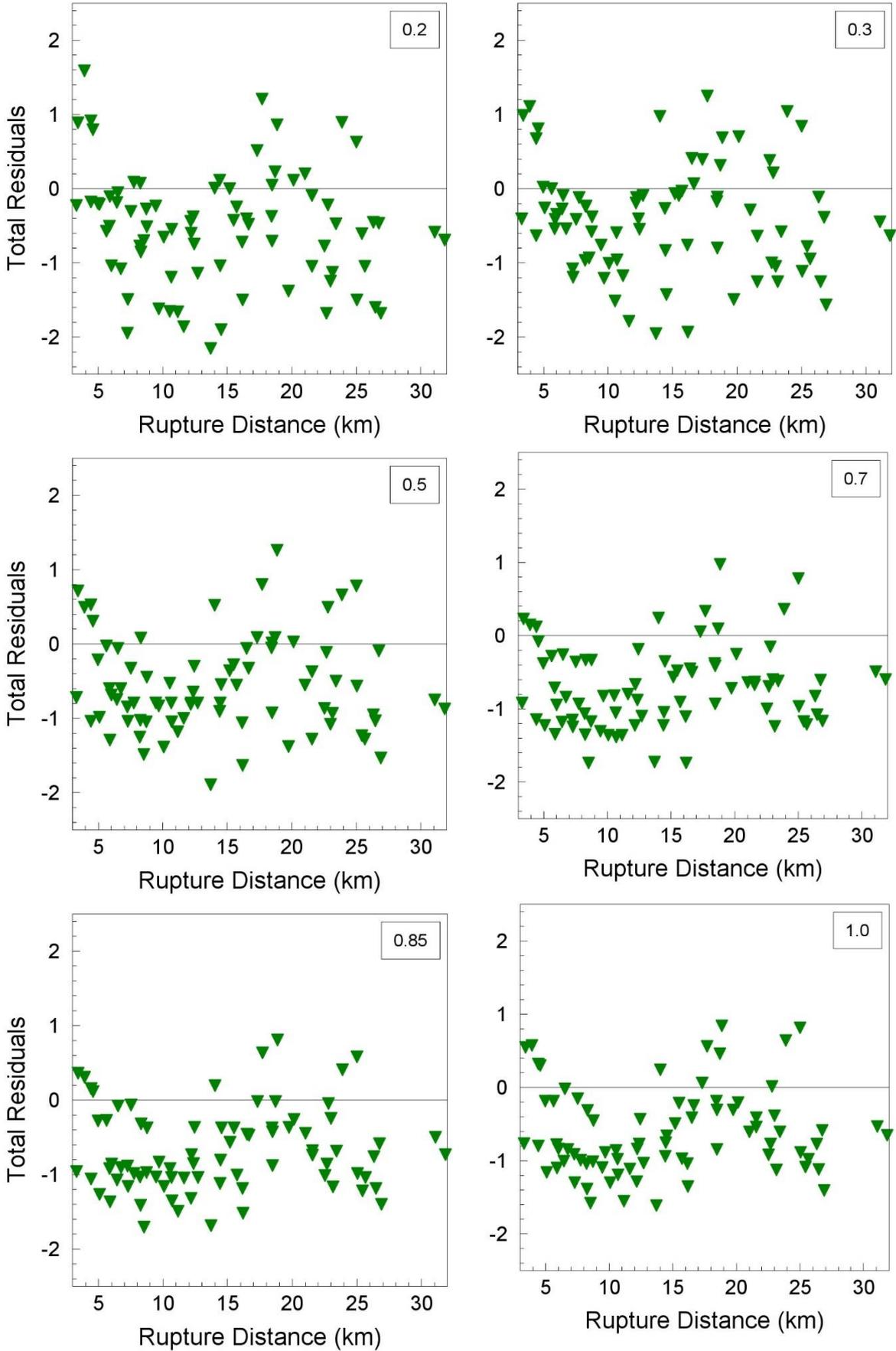
Figure 16   Residuals of Sa(T) at six response periods, T, against distance

3.1.5 Concluding Remarks Ground Motion Measurements

The M_L 3.4 Zeerijp earthquake of 8th January 2018 has contributed a large body of ground motion recordings that will inform and enrich the ongoing work of developing hazard and risk estimation models. The largest component of PGA recorded in this earthquake is 0.11g, which exceeds the previous maximum of 0.08g recorded in the 2012 M_L 3.6 Huizinge earthquake. However, the largest value of PGV—which is generally considered a better indicator of the damage potential of the motion—recorded in this latest event is 3.19 cm/s, which is smaller than the value of 3.46 cm/s recorded in the Huizinge earthquake. Moreover, the duration of the new maximum PGA is just 0.43 seconds; the duration of the 0.08g component from Huizinge was 0.52 seconds, also very short but fractionally longer.

An important observation is that the motions recorded in the Zeerijp earthquake are broadly consistent with the predictions from the ground motion model currently deployed in the seismic hazard and risk modelling for Groningen at short (< 0.1 s) response periods. At longer response periods, the model tends to over-predict when compared to the recorded motions.

3.2   Determination of Hypocentre Location

3.2.1   Standardised Operational Method

Event locations as reported by KNMI are calculated using the first arrival times of the P waves at the geophone or accelerometer stations. In the calculations, a generalized 1D velocity model over Groningen is used. Using this method, results can be delivered very quickly, in an automated fashion. The vertical (depth) resolution however is rather poor; the events are therefore set at a fixed depth of 3 km, the average depth of the Groningen gas reservoir. The lateral positioning uncertainty is about 500 m, but can be as large as 1000 m, in the most unfavourable circumstances. These circumstances are determined by local geology (Zechstein salt geometry), the magnitude of the event (signal/noise ratio) and the number and position of stations that have 'seen' the event.

3.2.2   Full Waveform Inversion (FWI) method,

Using a so called Full Waveform Inversion (FWI) method, more accurate event locations can be obtained, as well as focal mechanism parameters. In the FWI method, not only the first arrival time picks of P waves are used, but the full recorded seismic signal, including the S-wave waveforms. With the aid of a detailed 3D local velocity model (derived from available 3D seismic data and sonic logs), a more accurate hypocentre location can be determined, including depth.

The focal mechanism of an earthquake describes the deformation in the source region that generates the seismic waves. In the case of a fault-related event it refers to the orientation of the fault plane that slipped and the slip vector. Strike, dip and rake are the 3 angles that describe this mechanism. Focal mechanisms are derived from a solution of the moment tensor for the earthquake, which itself is estimated by an analysis of observed seismic waveforms during the FWI.

Shell has adopted this FWI workflow to better locate the events from the KNMI catalogue. Also, KNMI is using this approach, albeit not in an operational environment yet. NAM obtains the results from these workflows from Shell and KNMI respectively.

The process starts with the KNMI catalogue in an area of 8x8 km around Zeerijp, with all events occurring between 01-01-2013 and 10-01-2018. See Figure 17. There are 79 events identified, with a magnitude between 0.1 and 3.4. These 79 events are plotted on the background of the dip map of the top reservoir depth map, see Figure 18. This way we can see how the event locations are positioned with respect to faults in the reservoir. On the dip map, the more intense black the faults are, the bigger the fault throw is.

Figure 19 shows the same picture as Figure 18, but with the bigger events (M ≥ 1.5) highlighted as blue dots. There are 21 events in that period and in that area, that have a magnitude ≥ 1.5.

Figure 20 shows 14 events that have been relocated by Shell using the FWI workflow. The difference with respect to the original KNMI locations range from 73 to 979 m. It shows that considerable differences can be expected when applying the FWI workflow also to other events, such as the Zeerijp M=3.4 event. This is seen in Figure 21A) and B), where we see the result of Full Waveform type inversion performed by Shell and KNMI. Both relocated positions now map on the smaller fault, just SW of the main Zeerijp fault. It appears that the tip of this small fault is the source of the Zeerijp M=3.4 earthquake.
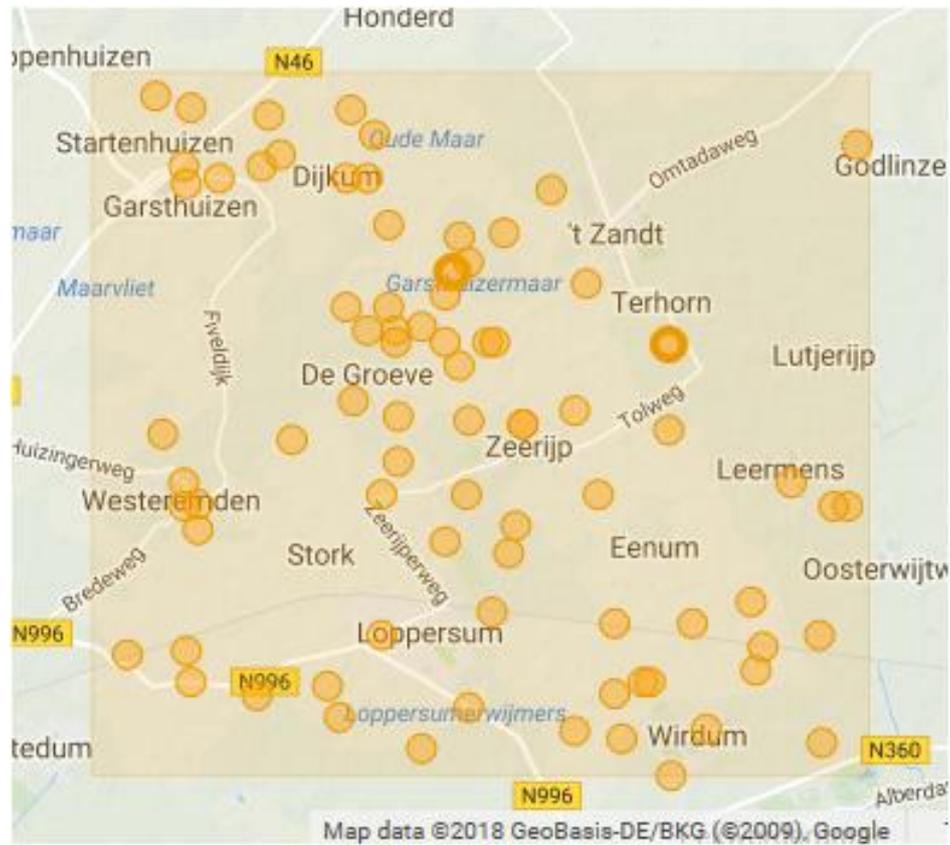
Figure 17   KNMI catalogue of 79 events between 01-01-2013 and 10-01-2018 in the Zeerijp area. Picture from KNMI seismic data portal website
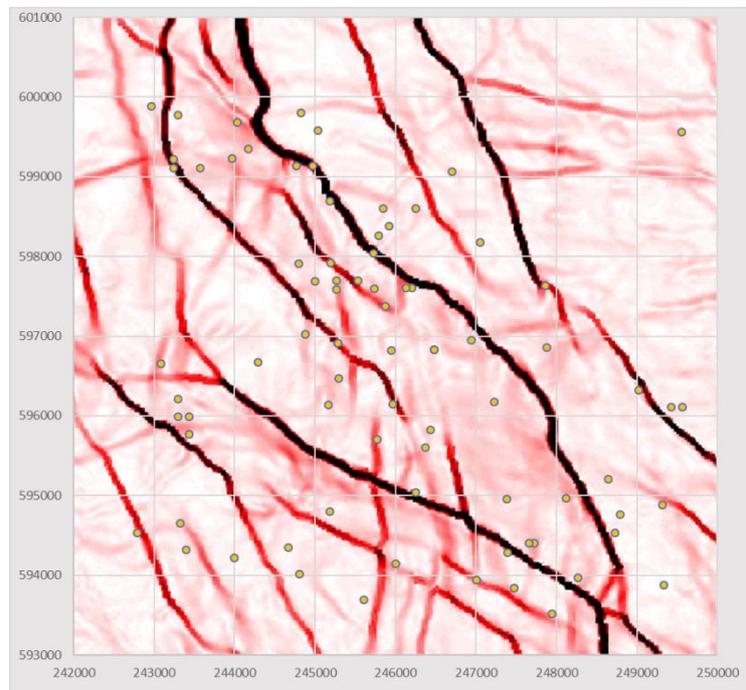
Figure 18   The 79 events plotted on the fault map (dip map of top reservoir) of Groningen field
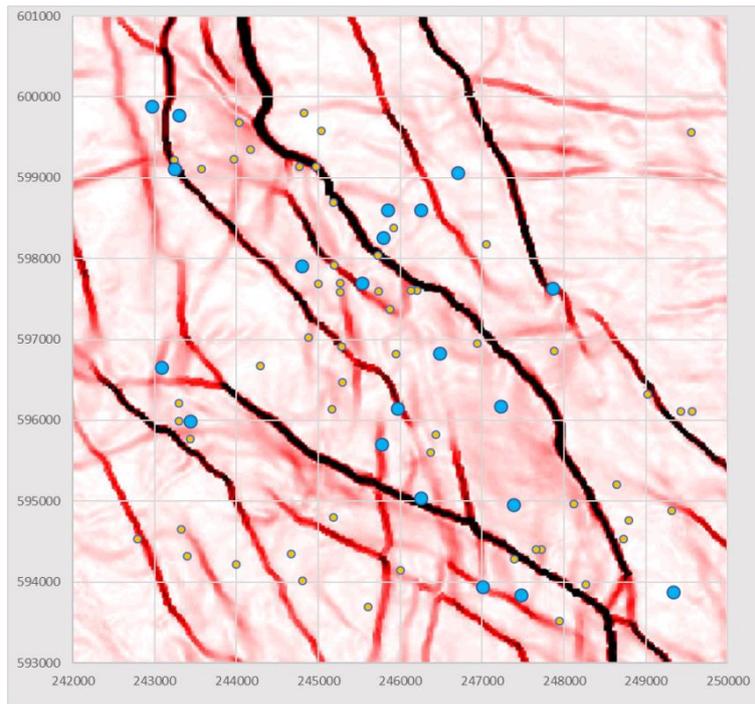
Figure 19   The 79 events plotted on the fault map (dip map of top reservoir) of Groningen field, with blue dots indicating the events with M ≥ 1.5
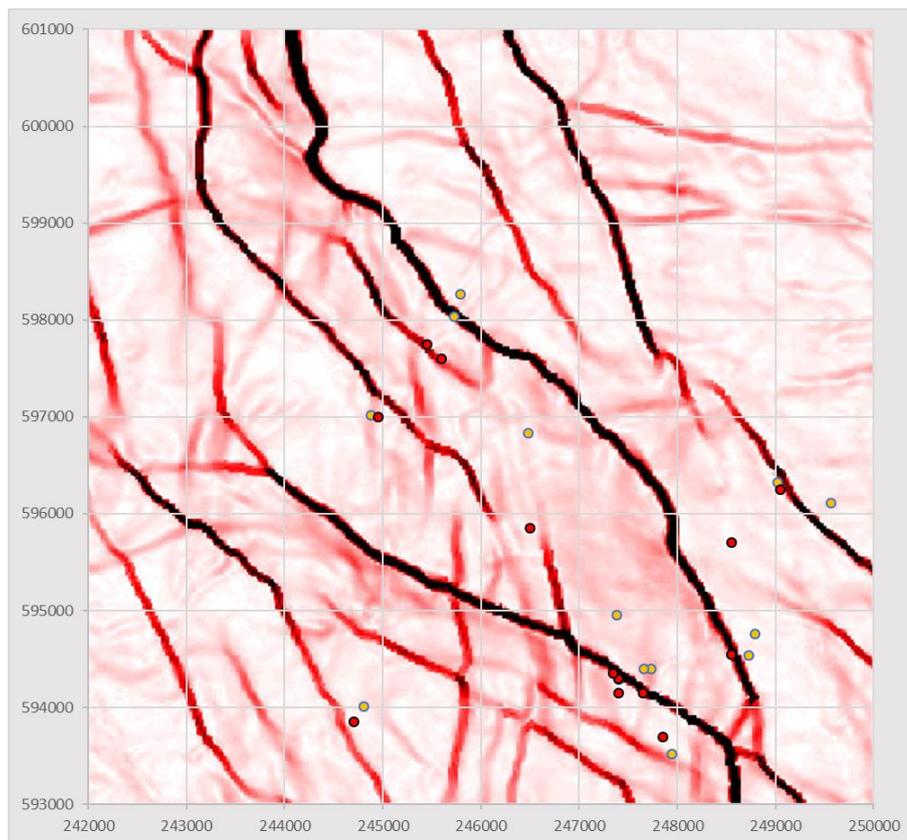
Figure 20   Original KNMI (orange dots) and relocated (red dots) events, subset of the catalogue of 79 events. Relocation done by Shell with Full Waveform Inversion workflow

Figure 21 shows the work done by KNMI on event (re-)location and focal mechanism determination. In blue are the following events: apart from nr 1, they all are from December 2017

Event nr	Date	Magnitude	Fault throw
1.	11-03-17	2.1	
2.	01-12-17	1.7	74
3.	06-12-17	1.8	
4.	10-12-17	2.1	34
5.	22-12-17	1.7	52
6.	29-12-17	1.4	92
ZRP	08-01-18	3.4	25

Table 1   Summary table of the 7 events near the hypocentre of the Zeerijp earthquake

All the 7 events are located on mapped faults and all show consistent focal mechanisms with respect to the delineation of the faults. Both event nr 5 and the Zeerijp M=3.4 event are positioned at the tip of the smaller fault just SW of the main Zeerijp fault, where event nr 6 is located.

One after-shock related to the Zeerijp M=3.4 event has been recorded by KNMI: on 09/01/2018 at 15:46:49 hours, with a magnitude of 0.7. This particular event has not been processed by the FWI workflow, so no precise coordinates of the hypocentre are available yet.

Figure 22 shows a cross section through the seismic data (in depth domain), perpendicular to the direction of the fault system. The hypocentre is located on a relatively small fault, with a minor throw, compared to both the adjacent faults.

As seen in Figure 21, the events numbered 2,5,6 and 4 are all positioned at different NW-SE trending faults in the Zeerijp area. Event nr 5 and the Zeerijp M=3.4 event are positioned on the same fault. The magnitudes of these events range from 1.4 to 3.4 and the fault throws ranges from an estimated 25 m to 92 m. There seems to be no relation between magnitude of the earthquake and fault throw. The event nr 6, with the smallest magnitude of 1.4 is at a fault with the biggest throw of 92 m, while the M=3.4 event is at a fault with only a 25 m throw. The fault throws mentioned here are all estimated values, obtained from seismic data.
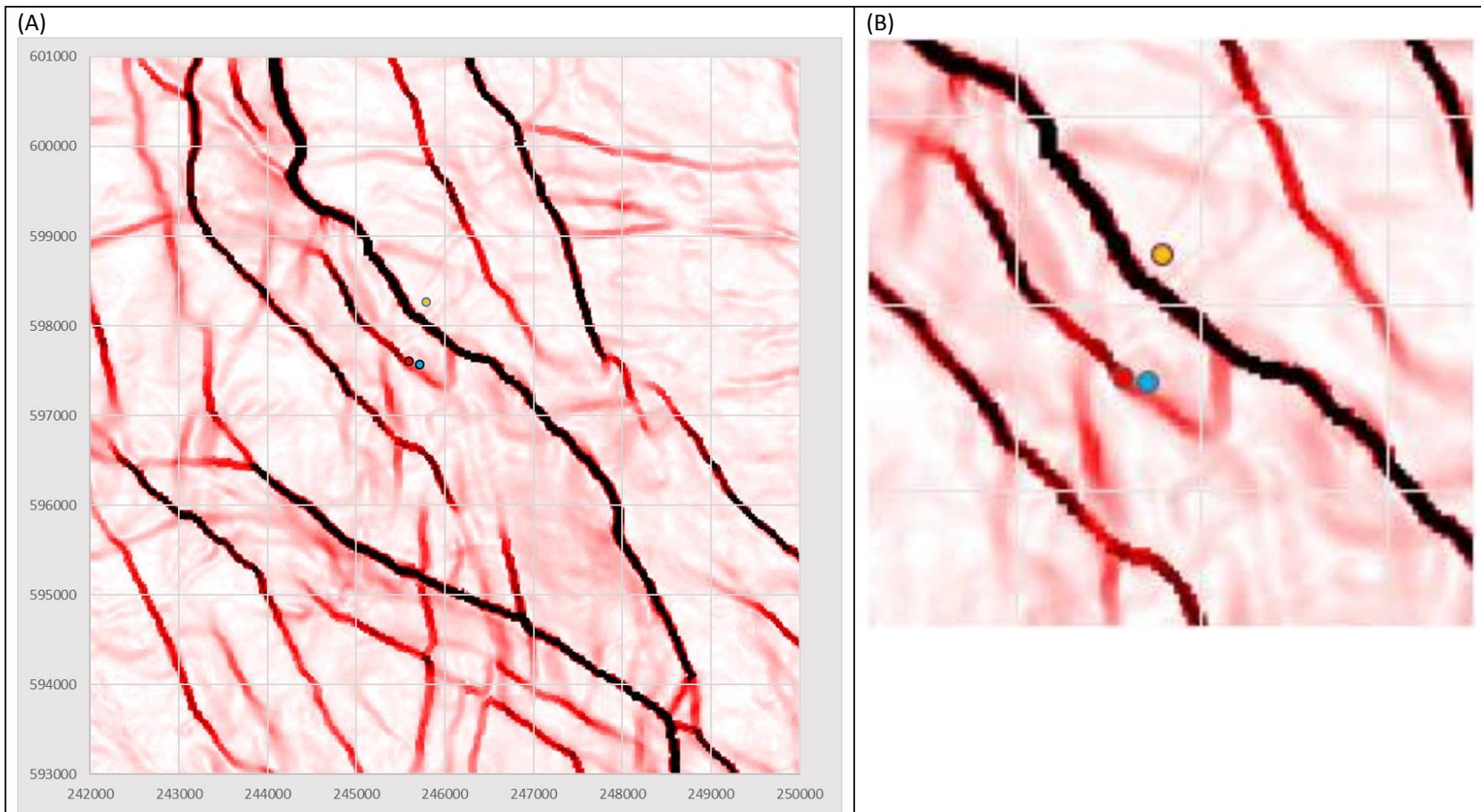
Figure 21   (A) Original KNMI location (orange dot), relocated by Shell (red dot) and relocated by KNMI (blue dot) of the Zeerijp M=3.4 event. Relocation performed with full waveform type inversions. (B) Zoomed-in. Observe the considerable lateral shift of 700 m of the new positions (red and blue dots) after FWI, compared to the original KNMI location (orange dot)
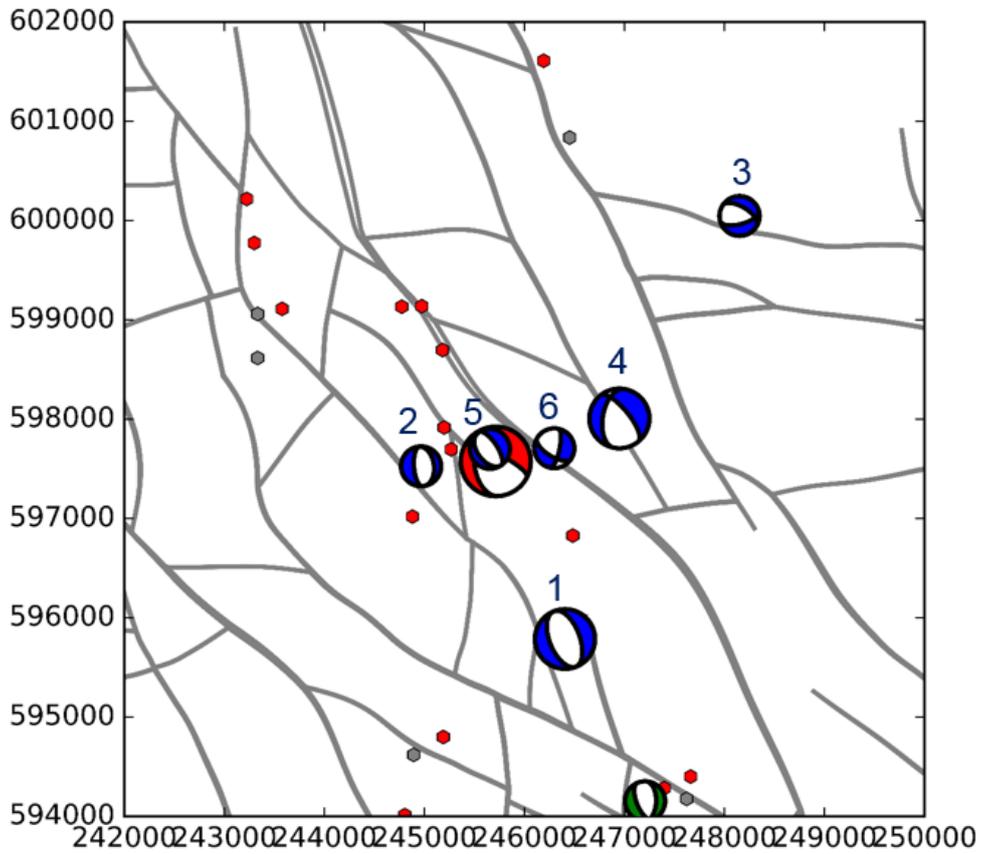
Figure 22   Picture from KNMI: locations and focal mechanism 'beach balls' obtained with FWI of 7 key events near Zeerijp. In blue the events from 2017, in red the Zeerijp M=3.4 event from 8/1/2018.
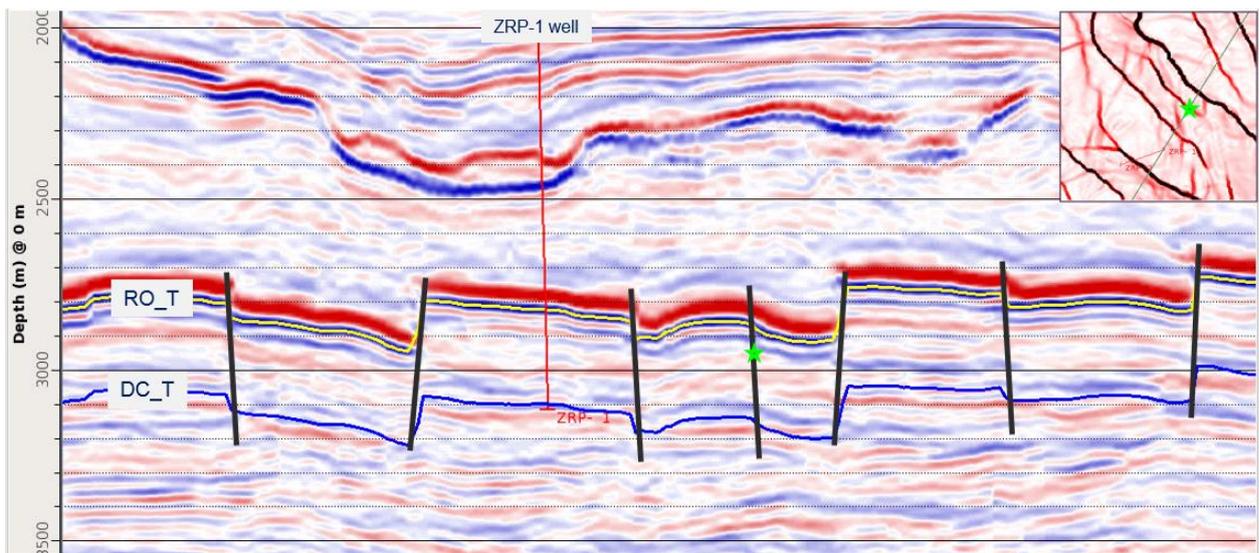
Figure 23   Cross section from SW (left) to NE (right), showing the position of the event at the green asterix. The throw of the fault it is located on is relatively small, compared to the bigger faults adjacent to it

3.2.3 Downhole geophone array

In the ZRP-2 well, at reservoir depth, an array of 12 geophones has been operational since 15/12/2017. This downhole array is intended to especially record events of lower magnitude and can record events as small as $M_L = -2$, provided the origin of this event is not too far away from the borehole. The Zeerijp M=3.4 earthquake was at a distance of about 2.3 km East of the ZRP-2 well.

Because the earthquake was stronger than those the geophones are set up to monitor, the signals recorded at the geophones are clipped. This can be seen in Figure 24.
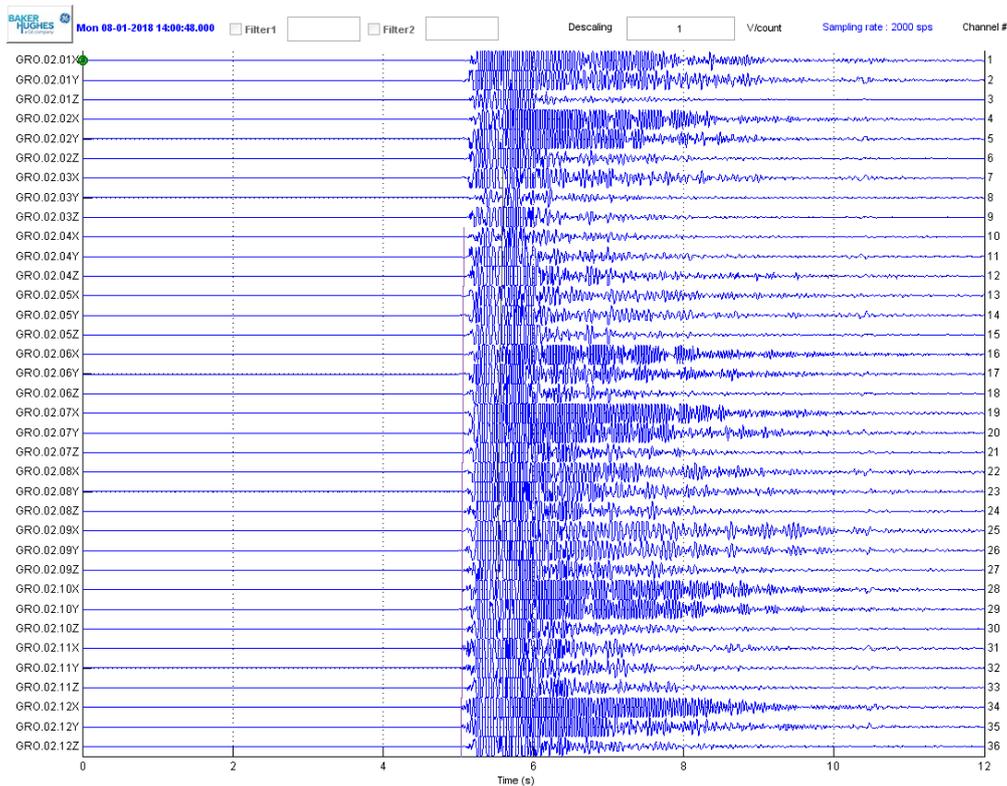
Figure 24   Record of the Zeerijp M=3.4 earthquake at the downhole geophone array at ZRP-2. At the top, geophone GRO.02.01 at a depth of 2808 m and at the bottom geophone GRO.02.12 at a depth of 3149 below NAP. Each geophone has three components, labelled X,Y and Z. The first arrival picks, marked by the line at around 5 sec, are clearly visible. The remainder of the signal is clipped.

Figure 25 shows a recorded aftershock event. Because this event is much less strong, a smaller part of the signals is clipped.
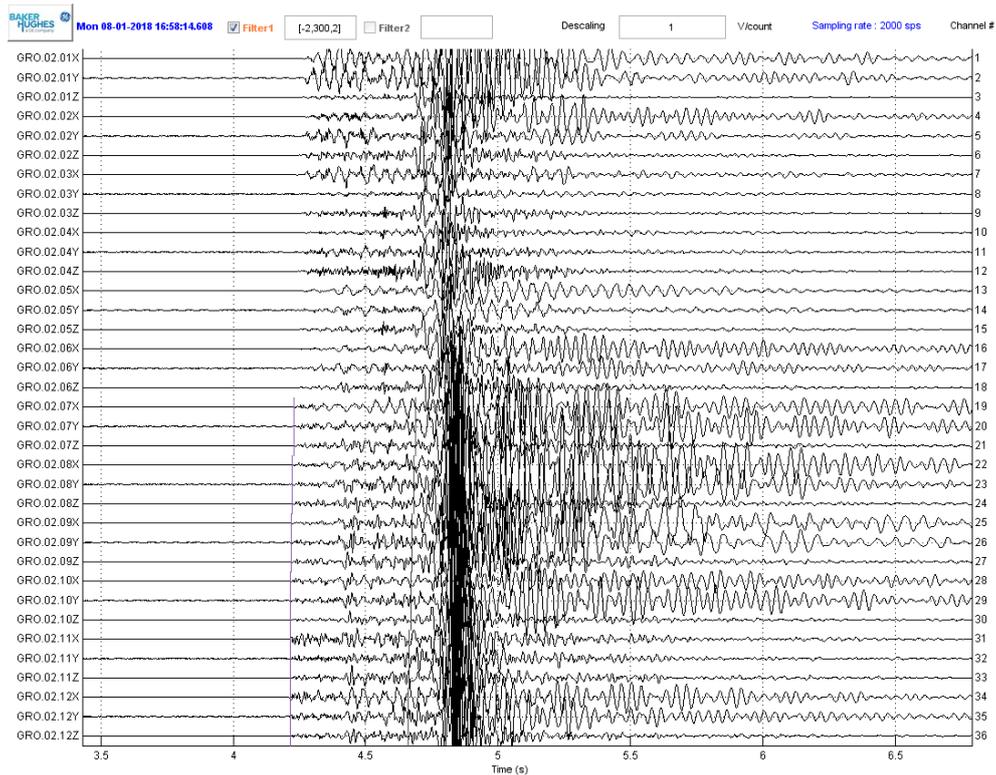
Figure 25   Recorded aftershock event, some 3 hours after the main event. Only part of the strong S wave energy around 4.8 s is still clipped.

The downhole array recorded events prior and post the main event. Table 2 gives an overview of the dates and times of these events. Some of these events were strong enough to have been recorded by te KNMI surface array as well.

|		locations by "Magnitude"			locations by KNMI			
Date	Time	RD-X	RD-Y	depth	Lat	Lon	depth	M
22-12-17	08:22:49,000							
22-12-17	19:40:29,064	246540	597880	2930	53,366	6,752	3,0	1,7
22-12-17	20:06:12,512	246480	597520	2900	53,357	6,75	3,0	0,4
22-12-17	23:41:02,020	246780	597940	3080				
24-12-17	07:05:14,768	246720	597700	2960				
25-12-17	03:40:39,584	246480	597640	2900				
29-12-17	09:00:02,609							
29-12-17	20:03:30,949							
29-12-17	23:15:48,780	246660	597760	2900	53,357	6,756	3,0	1,4
02-01-18	01:23:33,387	246900	598240	2900				
02-01-18	09:34:33,178	246534	597868	2936				
05-01-18	16:18:58,214	246480	597580	2900				
06-01-18	23:06:31,993	246300	597520	2900				
08-01-18	14:00:52,371	246180	597940	2900	53,363	6,751	3,0	3,4
08-01-18	14:03:38,722	246180	598000	2900				
08-01-18	14:08:40,041	246360	598060	2900				
08-01-18	14:13:45,703							
08-01-18	14:20:30,506	246360	598060	3050				
08-01-18	14:22:01,691	246480	597520	2900				
08-01-18	14:24:30,413	246300	597640	2900				
08-01-18	14:36:17,955	246540	597400	2900				
08-01-18	15:43:00,000							
08-01-18	16:58:18,180	246300	597520	2900				
08-01-18	19:16:28,635							
09-01-18	09:46:06,246							
09-01-18	15:46:49,503	246480	597340	2960	53,355	6,752	3,0	0,7
09-01-18	15:47:58,695	246540	597400	2960				
09-01-18	16:43:42,969	246600	597940	2960				
09-01-18	16:44:17,633	246360	598180	2930				
10-01-18	01:05:45,123	246600	597760	2960				
10-01-18	04:34:51,459	246480	598000	2900				
10-01-18	11:00:47,536							
10-01-18	16:05:17,710	246360	597820	2900				
10-01-18	18:44:36,386	246180	598000	2900				
11-01-18	18:52:55,932	246480	598000	2960				
12-01-18	14:18:02,915							
12-01-18	20:39:18,909							
12-01-18	22:39:04,732							

Table 2 Events detected by the downhole array at ZRP-2. UTC times are given. Where it was not possible to calculate locations, the line is blank. For some events, there is a correlation with the KNMI catalogue.

Figure 26 shows the cloud of locations of the events from Table 2 in the 3D model of Groningen around the ZRP-2 geophone well. Locations are provided by our contractor "Magnitude" and are not yet confirmed by Shell using the FWI workflow.
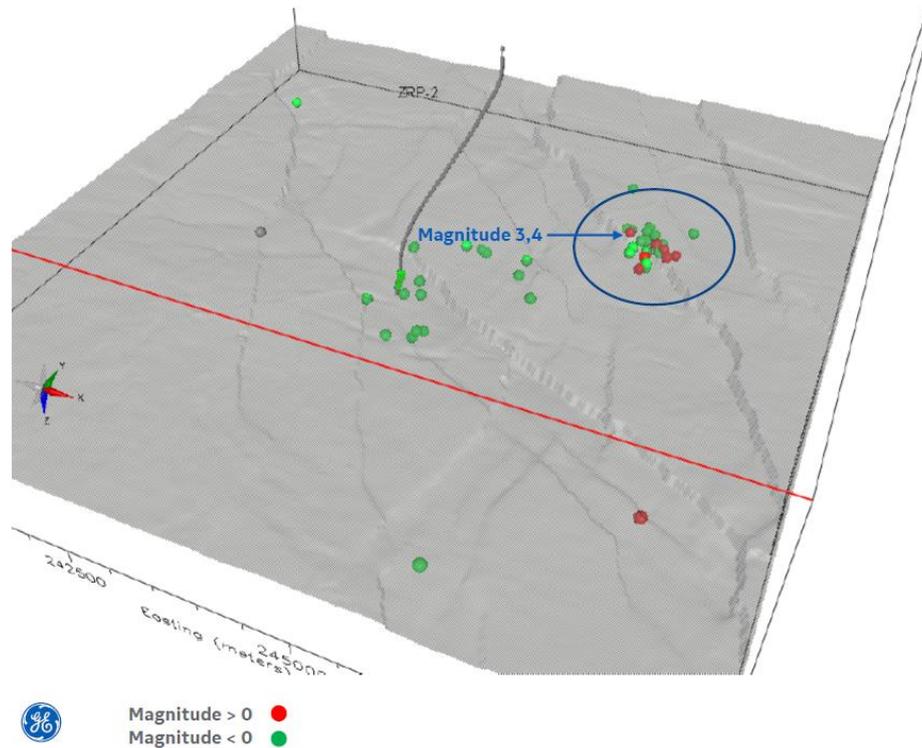
Figure 26   ZRP-2 well path (deviated) and the cloud of located events prior and after the main event on 8/1/2018, plotted inside the blue circle.

If we combine the results of the KNMI surface network with the ZRP-2 downhole array, we see in Figure 27 that the ZRP-2 determined locations are plotted around the main Zeerijp fault. This also holds for the original KNMI location. For the downhole array data, the locations are calculated mainly based on first arrival time picks of the P waves in a 1D average velocity model of the Loppersum area. As we have seen with the surface network data, this method has drawbacks with respect to accuracy. These drawbacks can be overcome by using Full Waveform Inversion (FWI) techniques. We intend to also apply this technique to the downhole recording and provide updated locations.
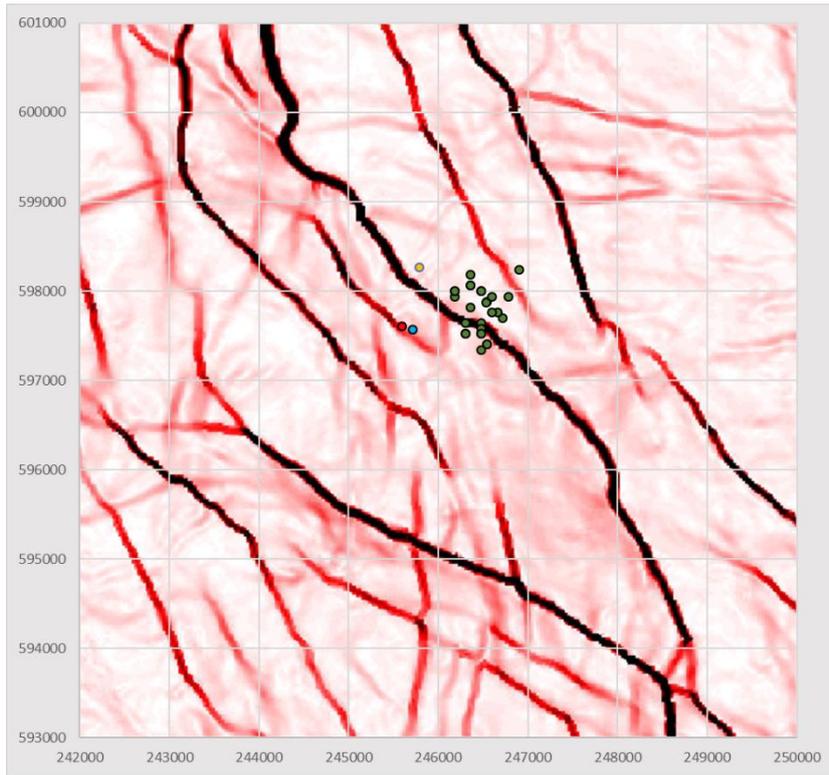
*Figure 27   Combined locations of the ZRP-2 downhole array (green dots), the original KNMI location (orange dot) and the re-
located positions by Full Waveform Inversion techniques by Shell (red dot) and KNMI (blue dot)*

3.3 Production and Pressures

Gas production from the production clusters in the direct vicinity of the Zeerijp epicentre was within normal operating conditions, and there have been no extraordinary production changes leading up to the seismic event on 8/1/2018 (Figure 28 and Figure 29). All nearby production clusters fall under the Loppersum regional production cap, and production rates were consequently restricted (stand-by rates).

Figure 30 shows a three-dimensional view from the dynamic reservoir simulator (NAM, 2017d), highlighting the epicentre location within the graben structure separating the Northwestern and Northeastern part of the field. There is some well control constraining the pressure match of the simulation model in the vicinity of the hypocentre. The Zeerijp-1 well (ZRP-1) was drilled in 1975 with RFT data acquired on 23/8/1975 . In addition, 28 downhole measurements of the pressure in the gas leg were acquired from ZRP-1 between 1977 and 2013. The Zeerijp-2 and -3 wells were drilled recently, and were RFT tested on 18/12/2014 and 19/8/2015 respectively. They have targeted the graben structure, and show a fairly uniform depletion within the aquifer leg. To the North of these Zeerijp wells lies the Oldorp well (OLD-1), located in the upthrown block to the West of the hypocentre. Between 1975 and 2015 there were 27 downhole pressure measurements acquired of the gas leg in OLD-1. Within the graben structure itself there is no well control to the North of the Zeerijp wells. Furthermore, at the hypocentre location the bulk of the reservoir sand lies below the gas-water-contact. Consequently, there is some uncertainty on the predicted pressures at the hypocentre location.

Figure 31 shows that the model is estimating gradual trends in reservoir pressure away from the production clusters, due to the dampening effect of a highly compressible fluid (gas) in a porous medium. Cross-section of pressure through the reservoir are given in Figure 32 and Figure 33. Figure 34 gives the pressure in time for the gridblocks across the suspect fault, and Figure 35 shows the associated depletion rate. It can be observed that at the fairly isolated location of the hypocentre (large distance to the production clusters) the pressure decline is very smooth.
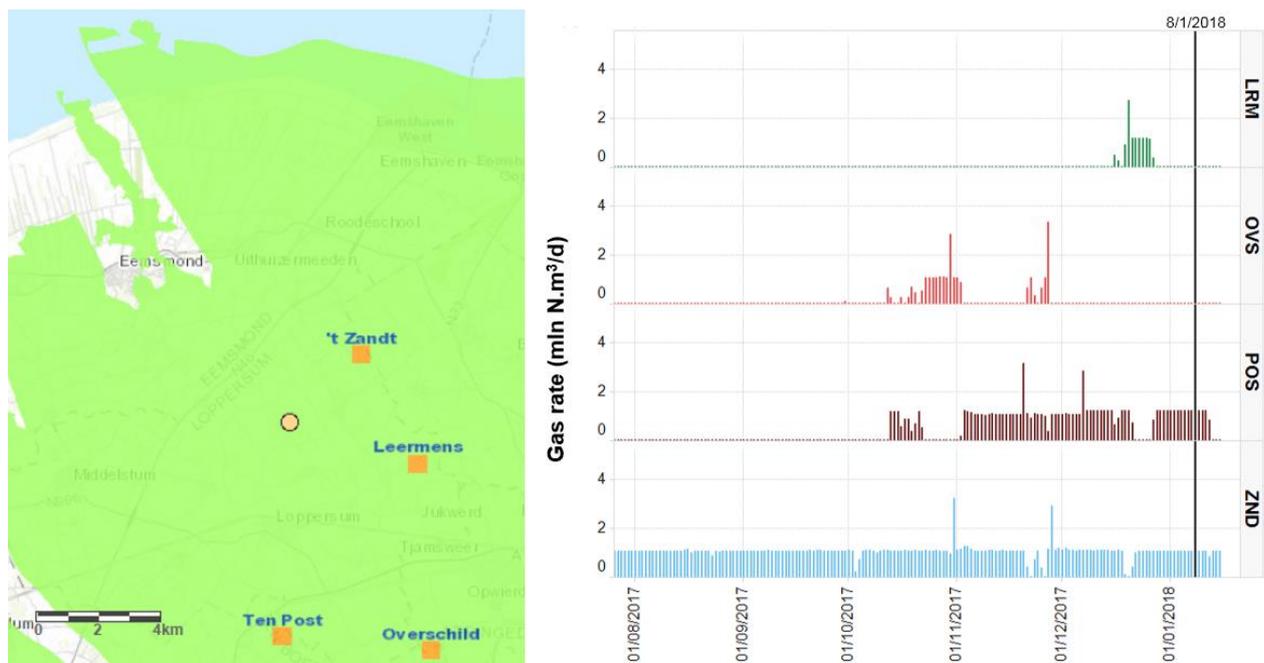
Figure 28   Daily production rates of clusters in the vicinity of the epicentre (yellow circle).
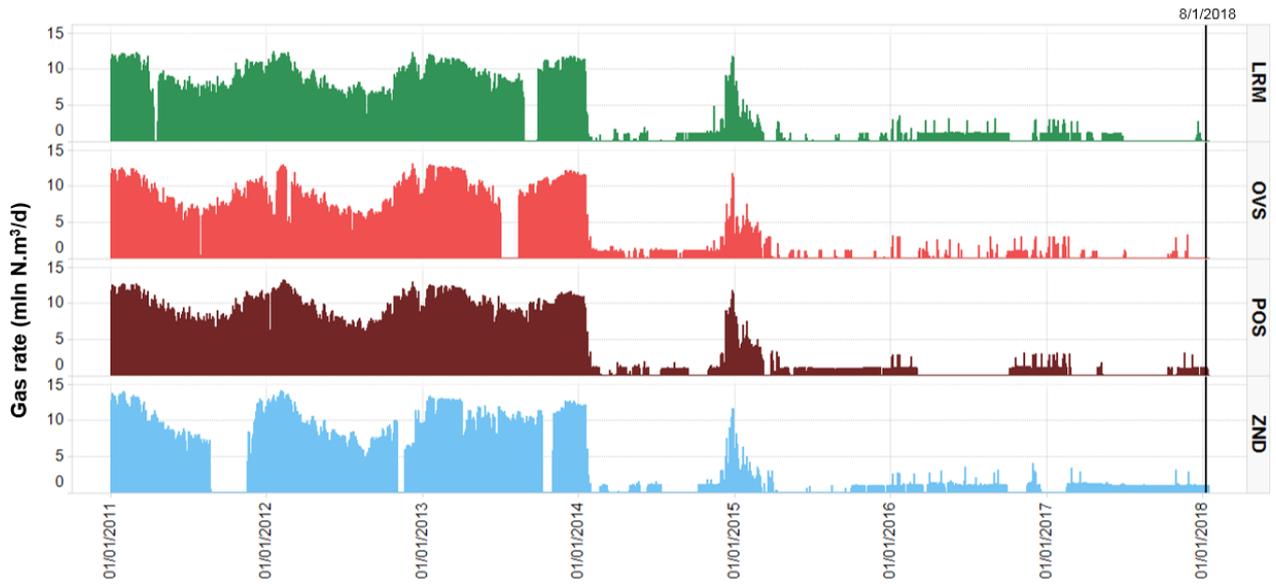
Figure 29   Longer term trend in daily production rates of clusters in the vicinity of the epicentrum
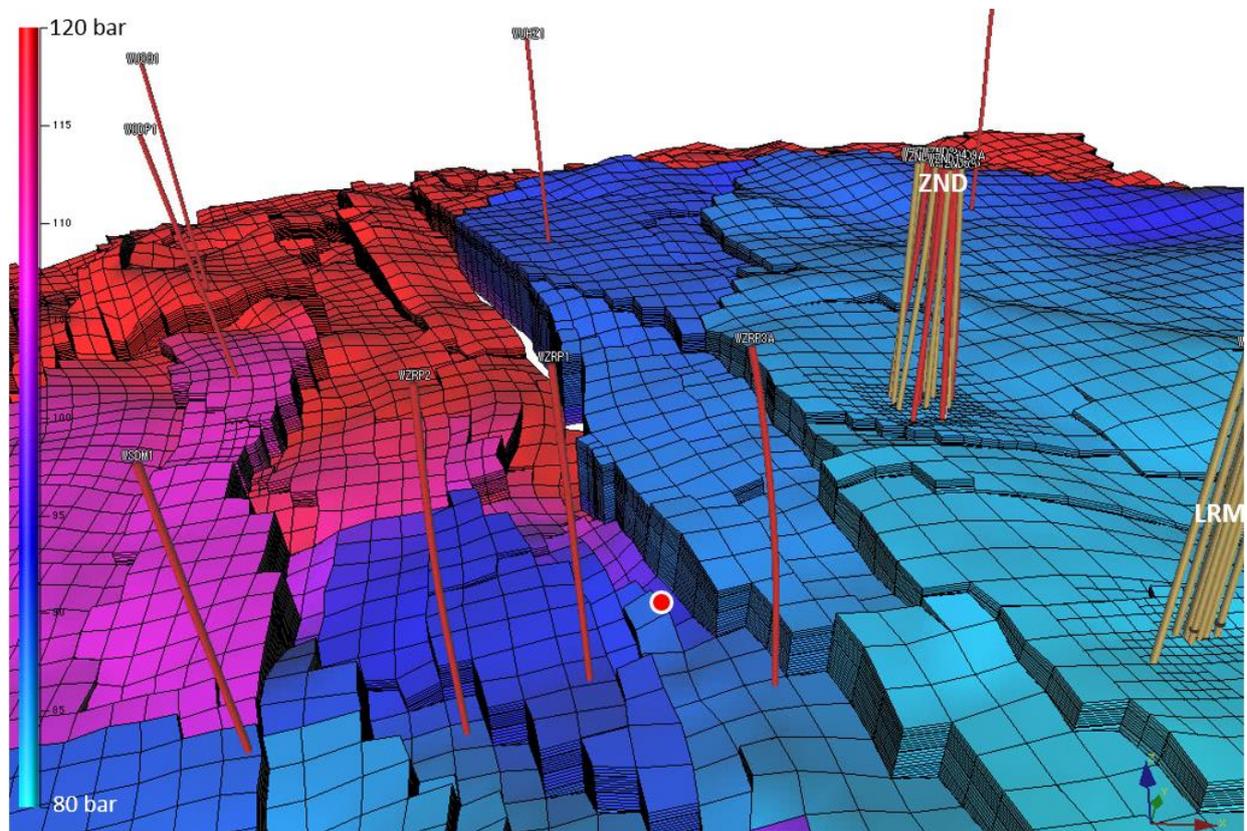
Figure 30   3D visualisation of reservoir pressure (8/1/2018) from the full field model (V4) in the top of the Slochteren formation. Colorscale clipped at 120 bar. Approximate epicentre location is indicated as a red circle
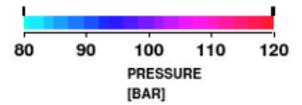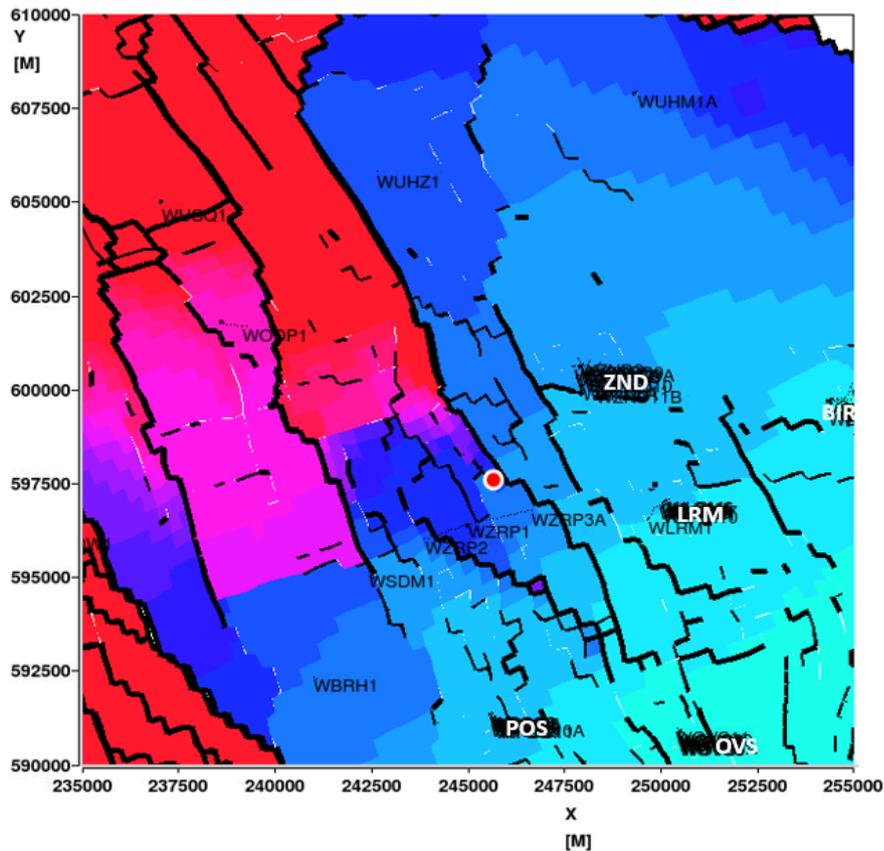
Figure 31   Reservoir pressure (14/01/2018) from the full field model (V4) in the top of the Slochteren formation. Colorscale clipped at 120 bar. Approximate epicentre location is indicated as a red circle.
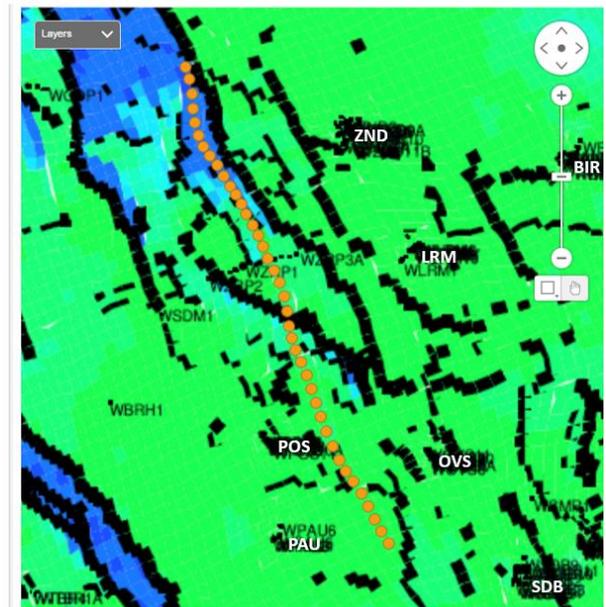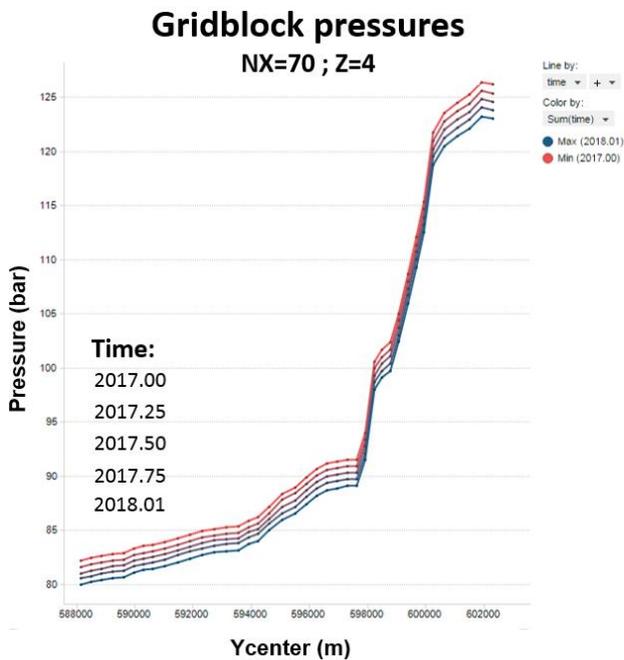
Figure 32   Pressure cross-section for NX=70 at yearly intervals
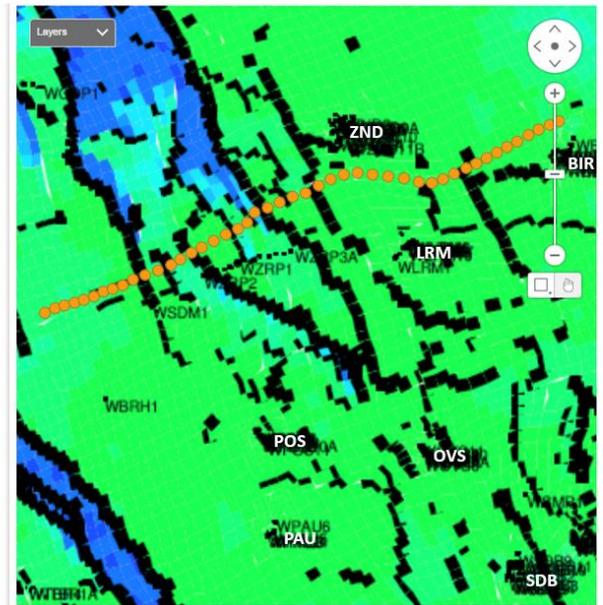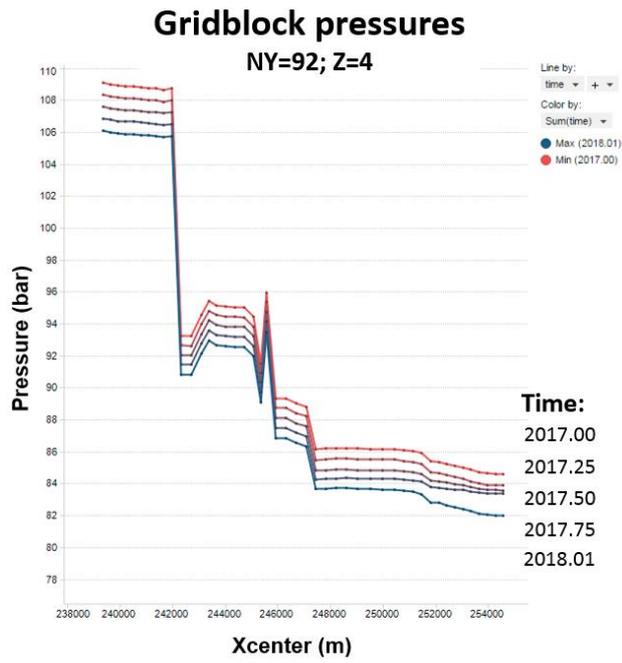
Figure 33   Pressure cross-section for gridblock NY=92, at yearly intervals
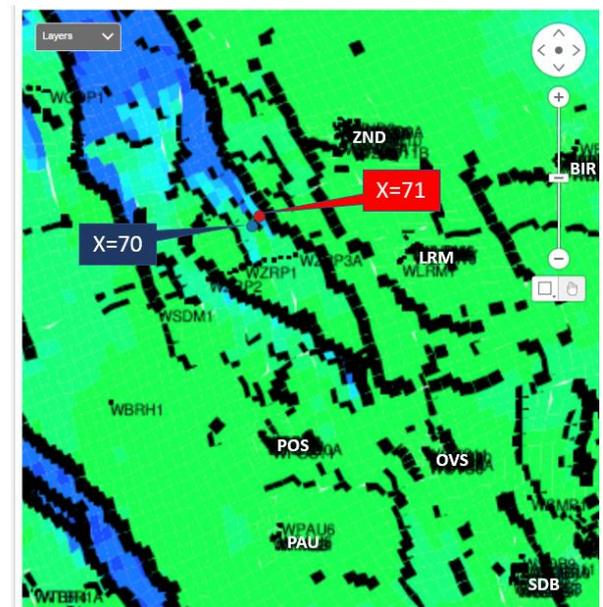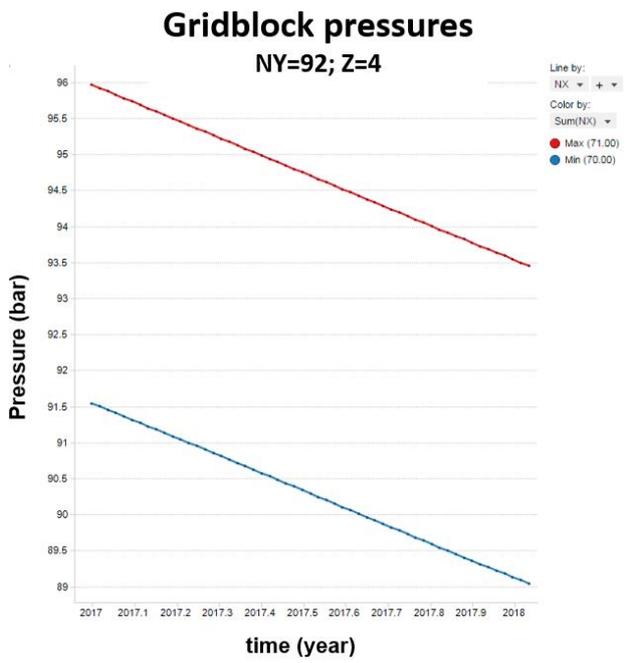
Figure 34   Gridblock pressures in time
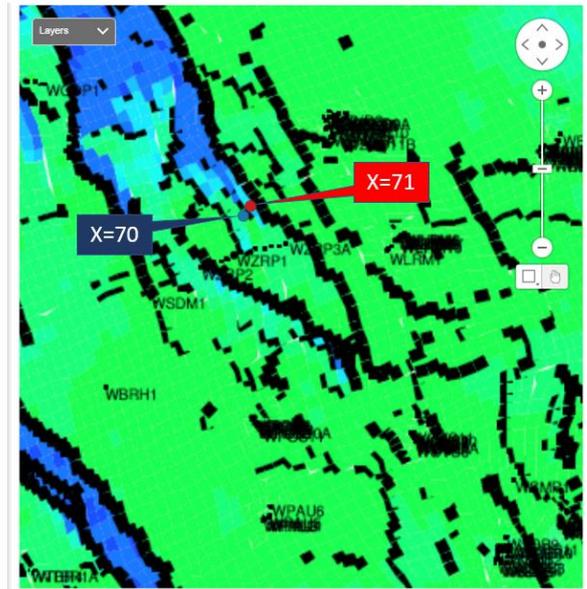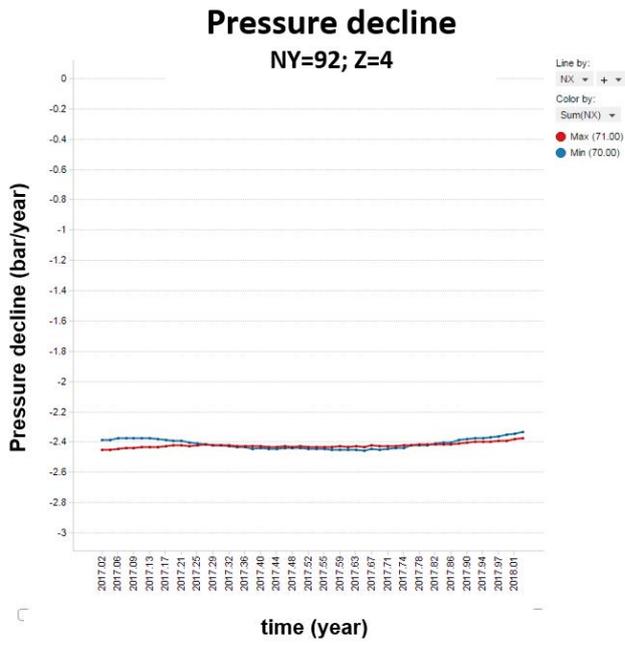
Figure 35   Gridblock pressure-decline (in bar/year) versus time

3.4 Reported Building Damage

An earthquake of the magnitude similar to the Zeerijp earthquake is expected to cause aesthetic damage (DS1) to buildings located near the epicentre. Buildings located at a distance from the epicentre of 10 km are exposed to a 0.1% chance of DS1 damage. At a distance of 3 km, buildings are exposed to a 10% chance of damage. These estimates are based on an evaluation of the ground motions and the TNO calibrated damage study (TNO, 2009) as described in chapter 8 of the recent Hazard, Building Damage and Risk Assessment of November 2017 (NAM, 2017c).

During the first 10 days following the Zeerijp earthquake, some 3,749 damage claims have been received by the CVW (Figure 36). On the first day after the earthquake (9th January 2018) the claim rate was highest with some 750 claims received in a single day. Currently, the claims rate is some 200 claims each day.

Figure 37 shows the damage claims around the Zeerijp epicentre. During the 10-days following the Zeerijp earthquake some 2,000 damage reports were received located in the area within 15 km from the epicentre. In comparison, during the 10-day period after the Hellum earthquake (of 30th September 2018, with a magnitude of M_L=3.1) some 1,638 damage claims were received. Damage claims are expected to further increase in the coming weeks. The current trend in damage reports and the level of damage is similar to those observed for other large earthquakes (since 2013).

The map of the damage claims prepared by CVW is shown in Figure 38. This map does not show an anticipated clear clustering of the damage claims around the epicentre of the earthquake. However, this is also in line with previous earthquakes, like for instance the Hellum earthquake of 2015 (NAM, 2016).
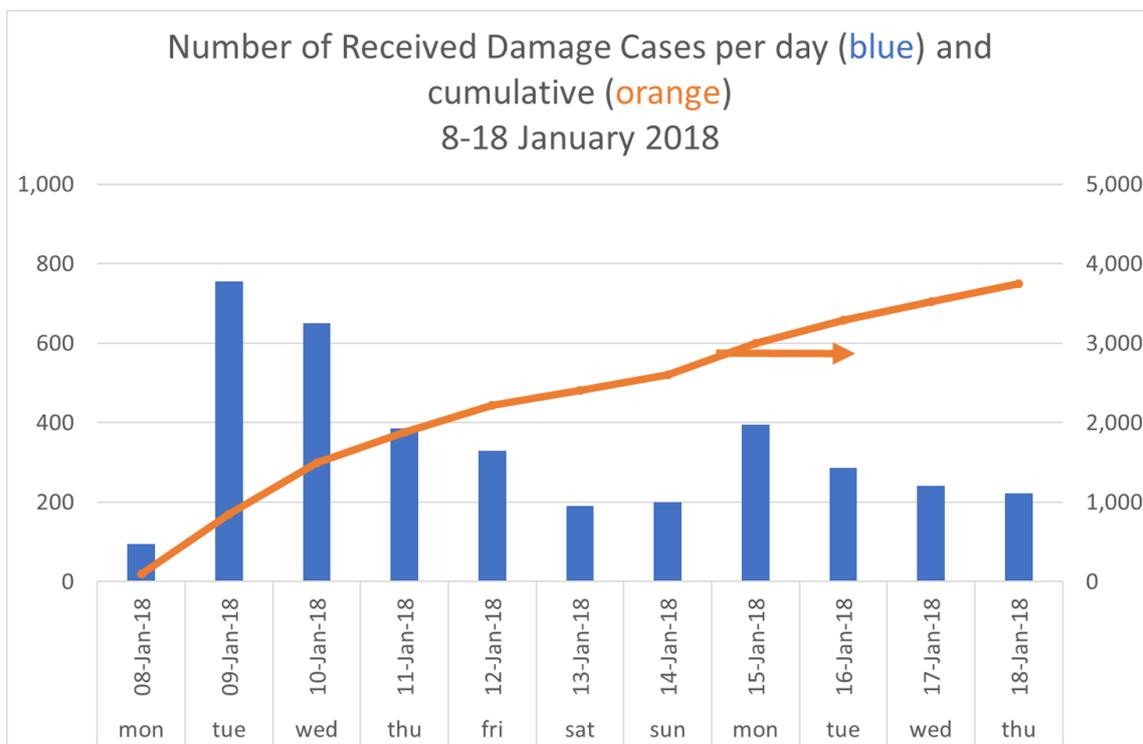
Figure 36   The number of damage claims received by CVW during the 10-day period following the Zeerijp earthquake.
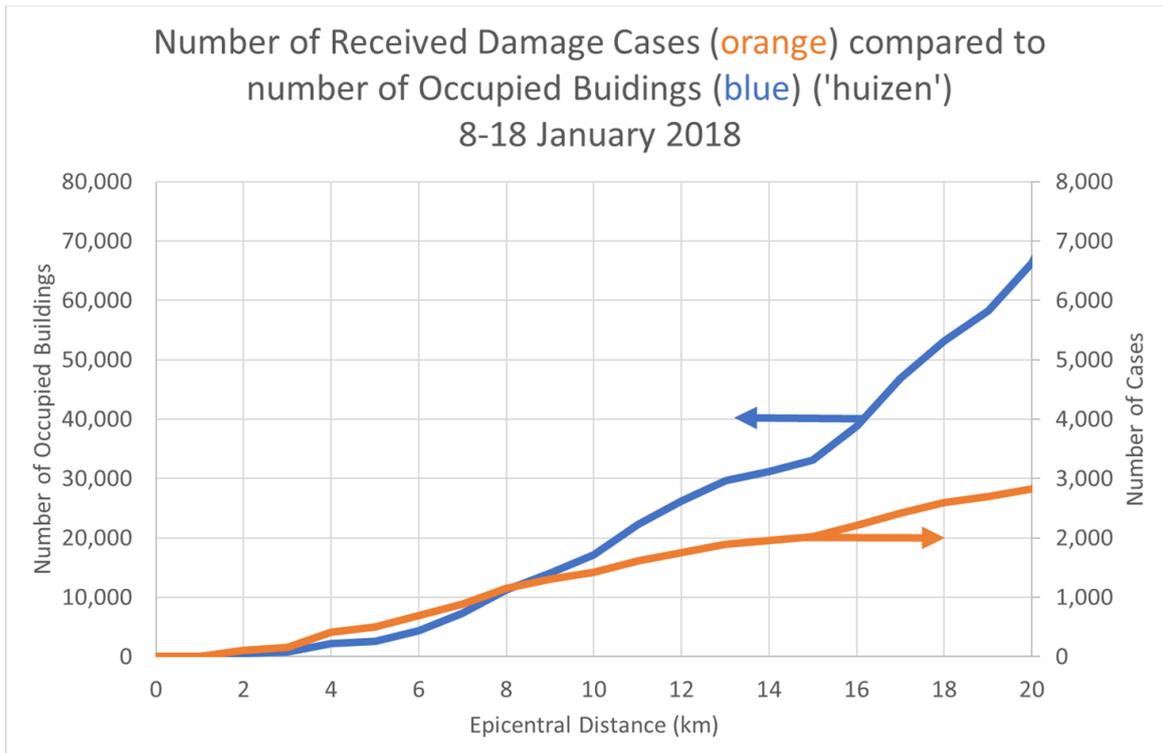
Figure 37 Number of received damage cases (schademeldingen) during the 10-day period after the Zeerijp earthquake (orange), compared to the number of occupied buildings (houses in blue) as a function of the distance to the Zeerijp epicentre.
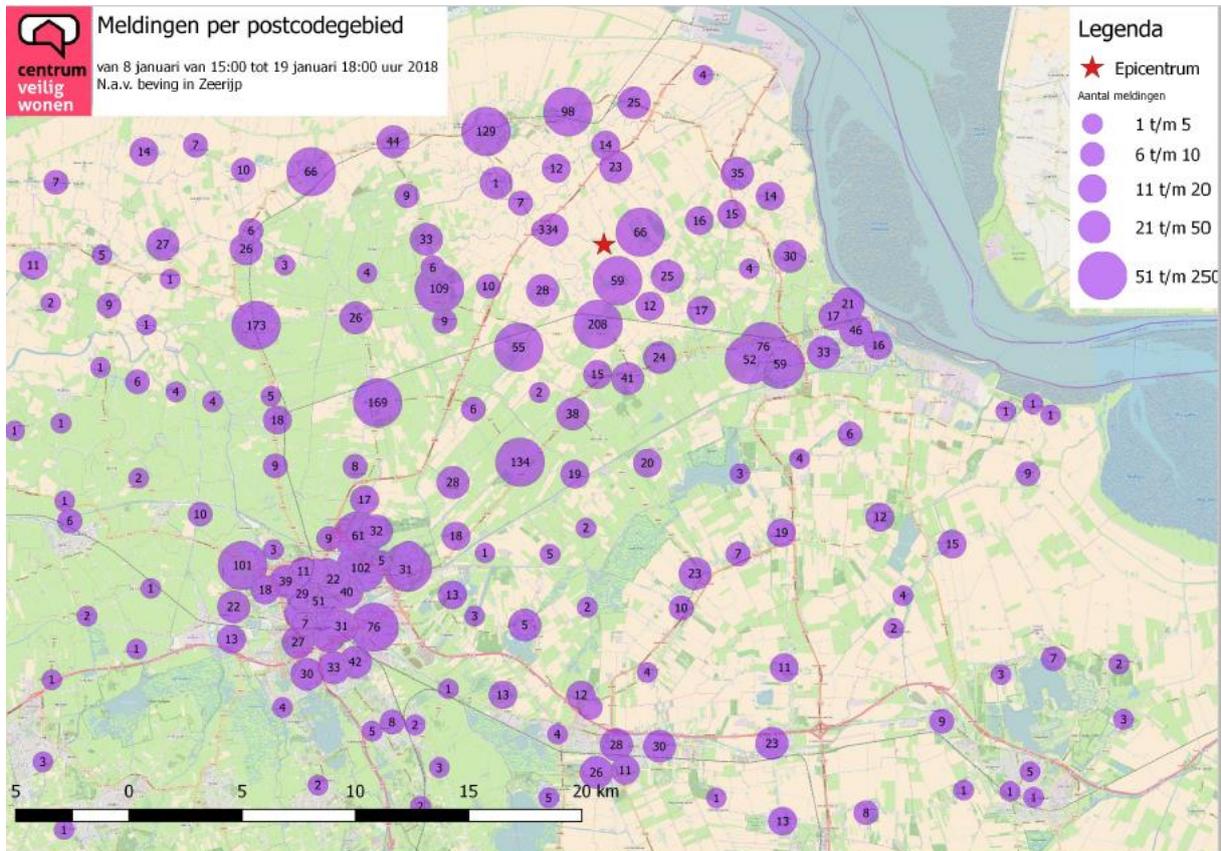
Figure 38 Map with the damage claims in the 10-day period from the earthquake (8-1-2018 15:00) to 6 pm on the 19th January 2018 as reported by the CVW.

A number of acutely unsafe situations (Acuut Onveilige Situaties; AOS) have been reported to CVW. In the first 10 days following the earthquake, some 100 residents contacted CVW, especially reporting feeling unsafe. The residents primarily reported cracks and requested an expert to assess the potential safety implications. No falling objects (e.g. chimneys) have been reported. Focus is on visiting these reported acutely unsafe situations within 24 to 48 hours and ensuring the situation is assessed and, for the cases identified to be unsafe, measures are taken to restore a safe situation. These visits therefore focus on ensuring safety and do not aim to identify the cause of the damage and unsafe situation. A study to identify the cause of the damage will be carried out later. Currently, insufficient research has been carried out to determine how many of these cases are the result of the Zeerijp earthquake. As of Wednesday 17th January, of the 99 reported acutely unsafe situations 90 resident had been visited. In 8 cases measures have been taken to make the situation safe.

No physical injuries, as a result of the earthquake, have been reported.

3.5   Conclusions

For the quality control of the hazard and risk modelling, it is important that we analyse the measurements and observations and identify any potential characteristics of the recent Zeerijp earthquake that do not fall within the anticipated frame of the modelling, which could prompt a potential re-evaluation of this modelling. The MRP (NAM, 2017a) in section 10.4, sets out this quality assurance process (Figure 39).
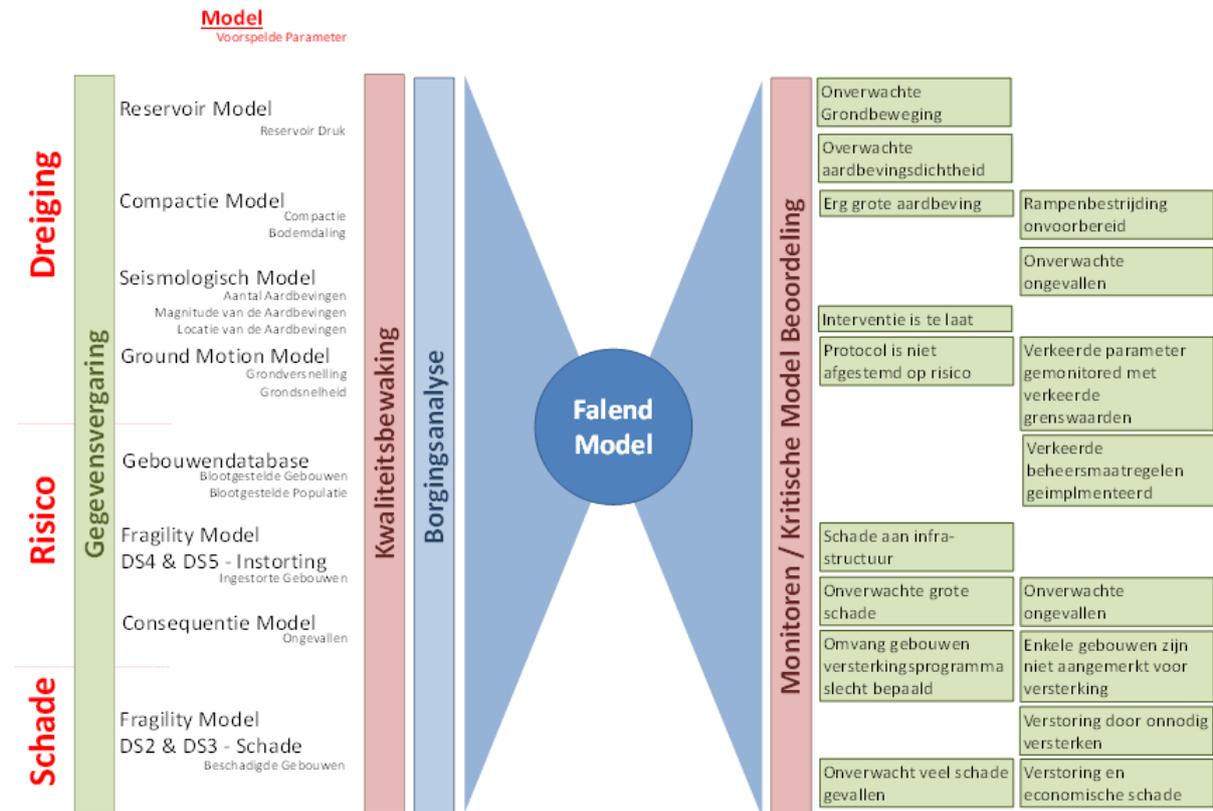
Figure 39   Cause/effect diagram for failures in the hazard and risk model for induced quakes in Groningen taken from MRP (NAM, 2017a) (Chapter 10.5, pg 36)

In this section of the Special Report (chapter 3), an overview and analysis of the measurements and observations of the Zeerijp earthquake is presented. This includes:

- intensity of the measured ground motions (both velocity and acceleration),
- duration of the ground motions,
- magnitude of the earthquake,
- hypocentre location of the earthquake relative the faults in the reservoir,
- building damage reported.

The assessment of the measurements and observations of the Zeerijp earthquake showed that in all aspects, the Zeerijp earthquake was within the anticipated range indicated by the hazard and risk modelling. No special characteristics of the Zeerijp earthquake, deviating from the modelling, have been identified.

In table 5.3 (on page 88) of the "Hazard, Building Damage and Risk Assessment – November 2017" (NAM, 2017e) the probability of an earthquake with a magnitude larger than M_L=3.6 during 2018, was

estimated at 16% (Figure 40). Some 5 years and 4 months have lapsed since the Huizinge earthquake of magnitude M_L = 3.6. The Zeerijp earthquake was in this respect therefore not an unanticipated or surprising event, and not outside the modelling frame.

The seismological model is used to forecast the seismicity in terms of, the number location and magnitude of future earthquakes. The probability of an earthquake with a magnitude exceeding a given magnitude can be assessed. In table 5.3 the annual probability of an earthquake occurring with a magnitude exceeding the specified magnitude is given. For instance, the probability of an earthquake occurring in 2018 with a magnitude exceeding ML=3.6 (the magnitude of the Huizinge earthquake) is equal to 16%.

YEAR	M≥3.6	M≥4.0	M≥4.5	M≥5.0
2018	16.0%	6.6%	1.6%	0.4%
2019	17.0%	7.0%	1.6%	0.4%
2020	17.8%	7.5%	1.8%	0.4%
2021	19.3%	8.0%	1.9%	0.5%
2022	20.2%	8.7%	2.2%	0.6%

Table 5.3   Table with annual probabilities for occurrence of earthquakes exceeding a set magnitude.

The probabilities for the occurrence of an earthquake with magnitude ML≥3.6, have not changed since the assessment for Winningsplan 2013. For the larger magnitudes, there is a slight reduction in the probability of occurrence since the assessment for Winningsplan 2013. Over time, these probabilities slightly increase when the field is produced at a constant gas production rate. However, over these longer time a-seismic relaxation of stresses in the reservoir might reduce seismicity below this forecast, as this effect has not been included in the model.

Figure 40   Excerpt from the "Hazard, Building Damage and Risk Assessment – November 2017" (NAM, 2017e) showing table 5.3 on page 88 of this document. These probabilities are based on a production scenario of 24 Bcm/year.

During the Zeerijp earthquake the largest PGA ever observed (resulting from an earthquake in Groningen) was measured. This PGA was also larger than the largest PGA measured during the Huizinge earthquake in 2012. However, the Huizinge earthquake was observed by only 7 accelerometer stations of the KNMI. Since then the KNMI network has been extended and the Zeerijp earthquake was observed by 79 accelerometer stations of KNMI. This is a more than 10-fold increase in the number of observations. The chance that one of these stations is located in the near vicinity of the epicentre and therefore picked up the highest PGA is therefore also much larger (Figure 3). This explains why, despite the lower magnitude of the Zeerijp earthquake, a largest PGA observed during the Zeerijp earthquake is higher than the largest PGA observed during the Huizinge earthquake.

The observed ground motions were within the predictions of the Ground Motion Model (GMM). The observations showed the same short durations and the same strong negative correlation between PGA and duration.

The hypocentre of the Zeerijp earthquake was within the reservoir section near an identified fault. This fault has also hosted an earlier smaller earthquake on 22 December 2017, with a magnitude of M_L = 1.7. However, there does not seem to be an extraordinary clustering of earthquakes on this fault.

The number reports of damage to buildings received by CVW are larger than after the Hellum earthquake in 2015, with a magnitude M_L=3.1, but within the expected range. Also, the large area where damage is reported falls within the observations after the Hellum earthquake.

No falling objects (e.g. chimneys) or injuries have been reported.

4 MRP status 8th of January 2018

The current status of the MRP is shown in Table 3. The status of the MRP is used to provide an overall assessment of the current (seismic) situation and this status is used in chapter 5 to discuss the expected merit of potential intervention measures as provided in NAM's letter (NAM, 2018b). The reason for writing this report is the exceedance of the PGA parameter at intervention level due to the Zeerijp 3.4 earthquake on January 8th. In this chapter, all other parameters of the MRP are discussed as well, to provide the necessary context in which intervention measures will need to be considered (see chapter 5).

MRP status			Grenswaarden		
	8 January 2018	1 January 2018	Waakzaamheid	Signalering	Interventie
Activity Rate (# aardbevingen, M ≥ 1.5)	19	18	15	20	25
EQ density (aantal x km^{-2} jr^{-1}, M ≥ 1)	0.38	0.34	0.17	0.25	0.40
PGA (in "g", laatste M2+)	0.11 (Zeerijp)	0.01 ('t Zandt)	0.05	0.08	0.10
PGV (meest recente maximum, in mm/s)	32 (Zeerijp)	0.9 ('t Zandt)	5	50	80
Damage State	No DS2 observed (yet) – more claims than calculated	-	Δ (model, actual)		
Other patterns	Loppersum M≥1 trend	Loppersum M≥1 trend	"Expert Judgement"		

Table 3   MRP status on January 2018. PGA, PGV and DS are MRP parameters that are adjusted on the basis of individual earthquakes (and hence can prove volatile), whereas Activity Rate and EQ density indicate longer-term (annual) trends.

The activity rate has increased to a level somewhere below the signaling level. Earthquake density has been fluctuating over the last couple of months around a value of about 0.29 km^{-2}yr^{-1}, but is now close to the intervention level with a value of 0.38 km^{-2}yr^{-1}. The maximum PGA associated with the Zeerijp earthquake was 0.11 g and crossed the intervention level. The PGV associated with the Zeerijp earthquake was 32 mm/s and remained below the signaling level. There are no indications for an anomalous development in building damage. The Loppersum increasing trend in number of earthquakes was identified in earlier reports (NAM, 2017f and NAM 2017g), and has been signaled as an ongoing concern.

4.1   Activity rate

The Zeerijp earthquake caused the activity-rate to reach a value of 19, above the alertness level and just below the signaling level. Figure 41 shows the development of this parameter over the last year in the upper panel. The upper panel shows the observed 12-months number (blue line with blue circles). The lower right panel shows the evolution of this activity rate (12 months number) over a much longer period (from 2000 onwards) and shows that the current number is higher compared to 2016 but low compared to 2006 and 2012-2015.

Figure 41   Temporal evolution of the activity rate for the last 12 months. The activity rate has increased somewhat in the first part of 2017 and fluctuated around the alertness level (NAM, 2017a). Lower right panel shows development of activity rate over a much longer time-period (from 2000 to 2017). The green line and the lower left panel show the development of M≥1 earthquakes.

4.2   Earthquake density

The earthquakes that contributed to the current EQ density value of 0.38 $km^{-2}yr^{-1}$ are shown in Table 4 and Figure 42.

Location	Date	Magnitude		Location	Date	Magnitude
Zeerijp	08 Jan 2018	3.4		Kantens	21 Jul 2017	1.1
Zeerijp	29 Dec 2017	1.4		Rottum	14 May 2017	1.4
Zeerijp	22 Dec 2017	1.7		Stedum	03 May 2017	1.5
't Zandt	10 Dec 2017	2.1		Uithuizermeeden	13 Apr 2017	1.4
't Zandt	06 Dec 2017	1.8		Zeerijp	11 Mar 2017	2.1
Zeerijp	01 Dec 2017	1.3		Wirdum	26 Feb 2017	1.4
Zeerijp	01 Dec 2017	1.7		Zandeweer	26 Feb 2017	1.2
Kantens	15 Oct 2017	1.0		Loppersum	25 Feb 2017	1.3
Garrelsweer	27 Sept 2017	1.2		Zijldijk	19 Feb 2017	1.4
Zandeweer	01 Sept 2017	1.1		Startenhuizen	15 Feb 2017	1.6
Appingedam	29 Aug 2017	1.8		Startenhuizen	12 Feb 2017	1.3
Garsthuizen	14 Aug 2017	1.2		Kantens	05 Feb 2017	1.3
Loppersum	25 Jul 2017	1.0				

Table 4   Earthquakes in the Loppersum area that contributed to the exceedance of the earthquake density threshold value.

45

This set of earthquakes shows (as expected) a large overlap with the set that contributed to the exceedance of the earthquake density late last year (NAM, 2017g). And that is in turn the result of the Quartic Kernel methodology chosen, using a fairly large search-radius and time horizon including earthquakes from within a circle with a radius of 5 km for a period of about a year.

This choice of calculation method (and MRP threshold values) for EQ-density leads to a deliberate early and potentially often triggering of this MRP parameter with the intent of early picking up signals of changing subsurface conditions (the other intent of this parameter is to simply pick up an increase of concentration of earthquakes in a certain area without special underlying cause but potentially causing nuisance nevertheless). This means, however, that an exceedance of this earthquake density threshold always needs to be judged in the context of other seismicity developments; in this case the current value is related to the general increase in seismicity in the Loppersum area as already highlighted in references NAM 2017f and NAM, 2017g.
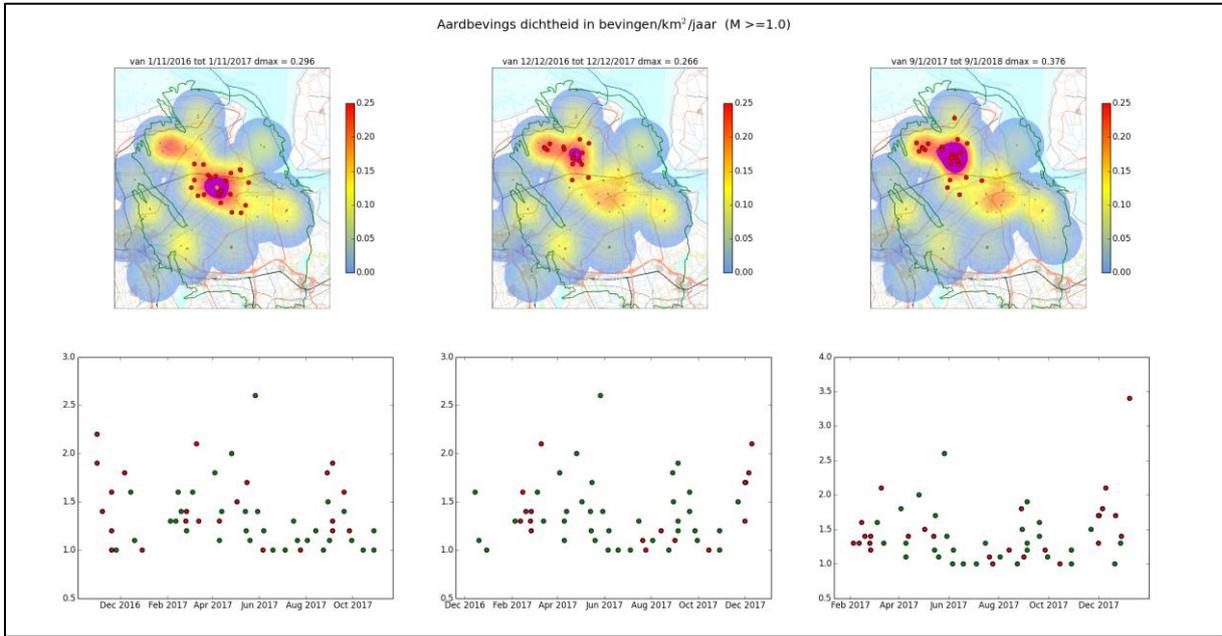
Figure 42   Earthquake density values for the Groningen Field. Colours indicate Earthquake density values. The red dots indicate the earthquakes that contribute to the exceedance of the signalling level.

Figure 42 shows the temporal development of earthquake density in the area. The upper panel with the three maps shows the evolution of the earthquake density for recent times over the Groningen field.

Figure 43 shows maximum values for specific locations over a much longer period and it shows that although the values for earthquake density have been increasing over the last year, values have been much higher around 2007 and 2014 for (e.g.) the Wirdum area.
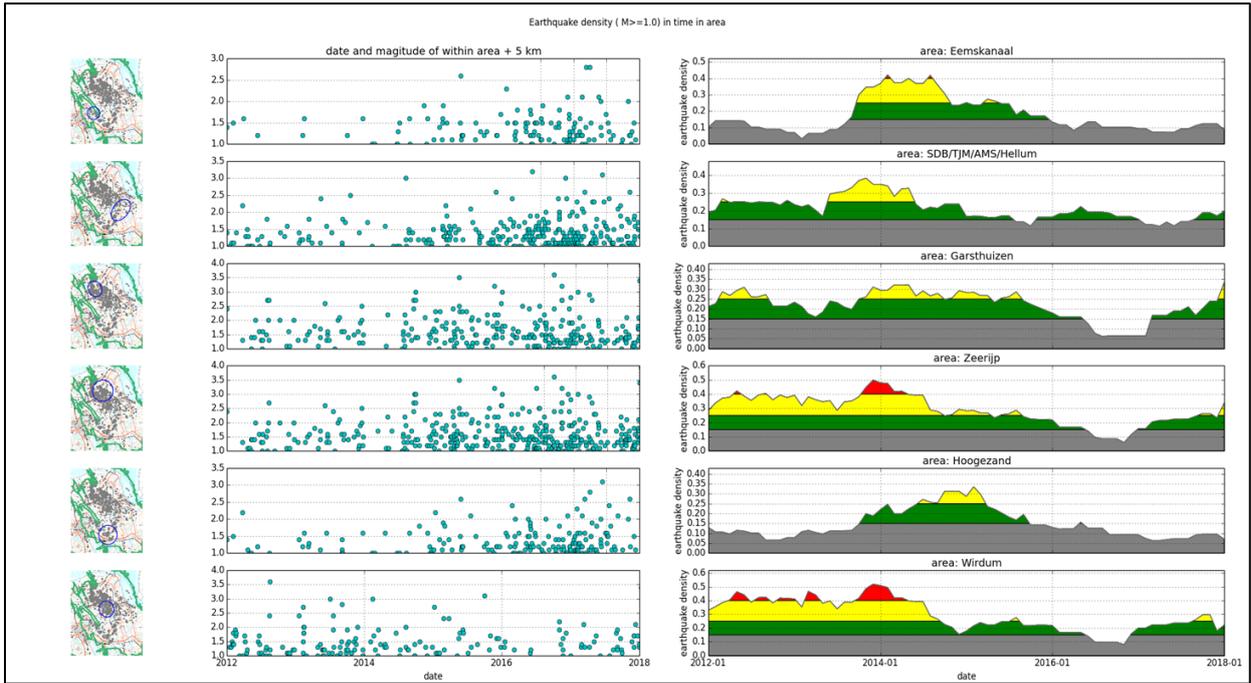
Figure 43   Evolution of the earthquake density map over time. Third panel from below shows the earthquake density development for the Zeerijp area.

4.3   PGA and PGV

Figure 44 shows the PGA value associated with the Zeerijp earthquake. It shows that this earthquake caused a relatively high measured PGA (0.11 g). As explained in the previous section, this is related to the 10-fold increase in the number of measurement stations, leading to a situation where the probability of having a measurement station close to the epicentre is higher (as happened for Zeerijp, but not for Huizinge for example). As shown in the previous figure (Figure 43), the Zeerijp highest recording was some 500 m from the epicentre, whereas for Huizinge that distance was about 1 km.
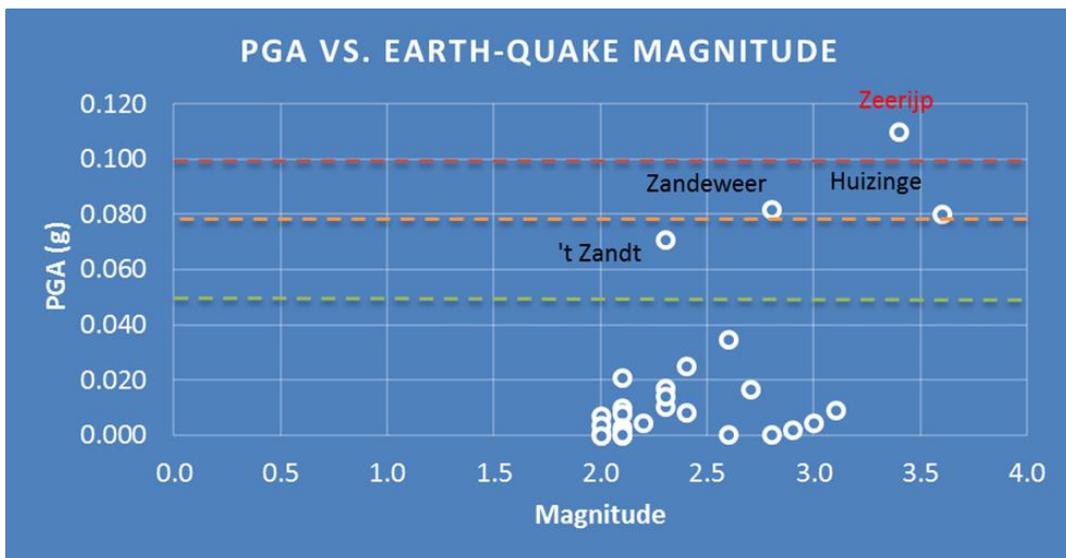
Figure 44   Plot of PGA values observed in the Groningen field (M≥2.0). The most recent Zeerijp earthquake is shown in red

Figure 45 shows the PGV value for the most recent Zeerijp earthquake. The PGV value of 32 mm/s remained below the signaling level (and is also unlikely to have caused any DS2 damage. However, the damage assessments are not yet completed).
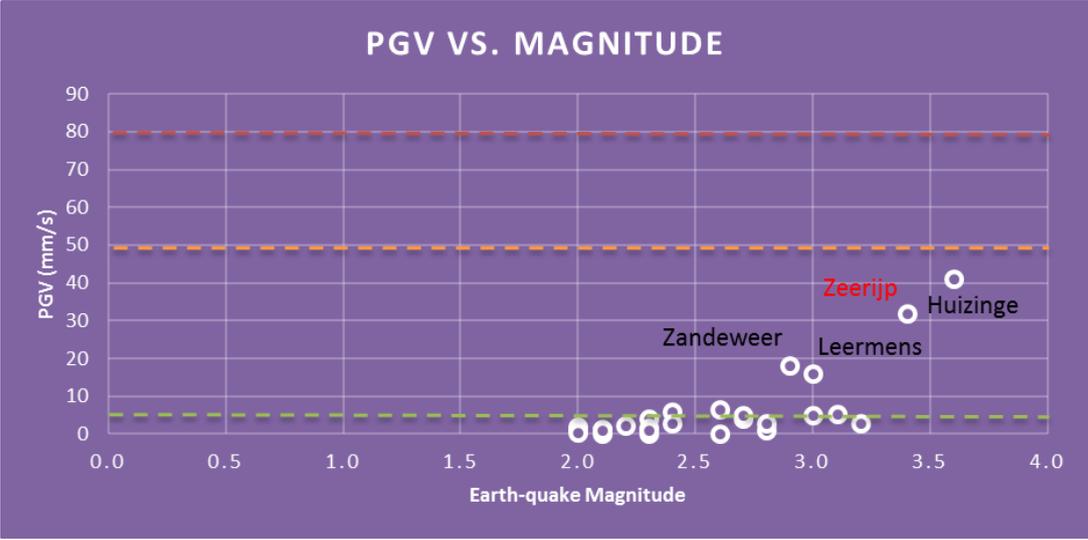
Figure 45   Plot of PGV values observed in the Groningen field (M≥2.0). The most recent Zeerijp earthquake is shown in red

4.4   Damage state

At this moment, no observations have been made to suggest that DS2 (structural damage) has occurred as a result of the Zeerijp earthquake.

4.5 Other patterns and considerations

4.5.1 Loppersum trends and forecasts

Figure 46 shows the number of earthquakes in the Loppersum and East areas for earthquakes with a magnitude of 1.5 and higher (NAM, 2017d). For both areas holds that the current seismicity level is low compared to 2011. The Loppersum area, however, shows a recent increase in seismicity (despite minimal production, see also NAM, 2017g for discussion). The East area, in contrast has not shown this upward increase.
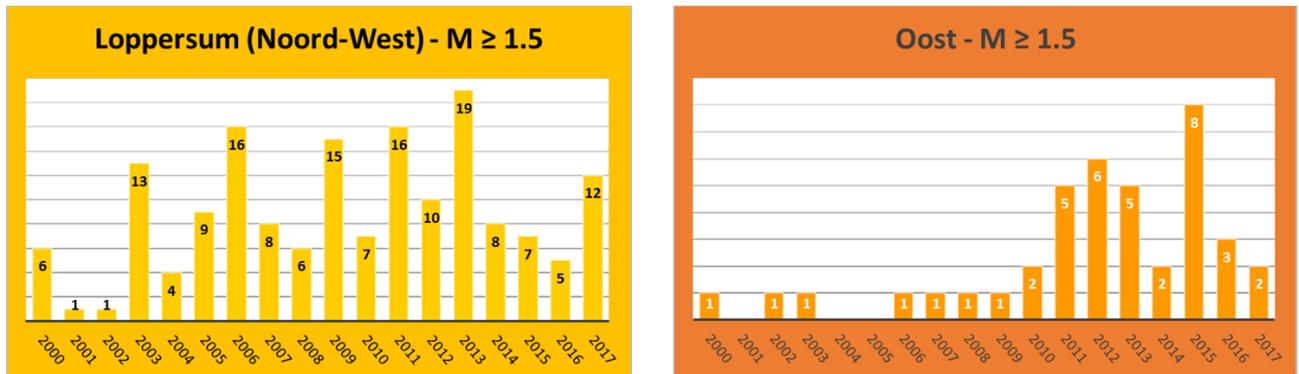
Figure 46   Yearly number of earthquakes for the Loppersum area and for area "East". The Loppersum area shows a recent increase whereas the "East" area still shows a relatively low number of earthquake (see also reference NAM, 2017f and NAM, 2017g).

Figure 47 shows the monthly numbers for the Loppersum area for two magnitudes in the upper two panels. The lower two panels show the forecasted number of earthquakes in the area (NAM, 2017f). The left lower panel shows a machine-learning ("Random Forest") forecast indicating a fairly flat, even somewhat declining base-case forecast (NAM, 2017g, for more discussion). The lower right panel shows a forecast from the hybrid geomechanical-statistical model showing a very slight increase of expected number of earthquakes for the area.
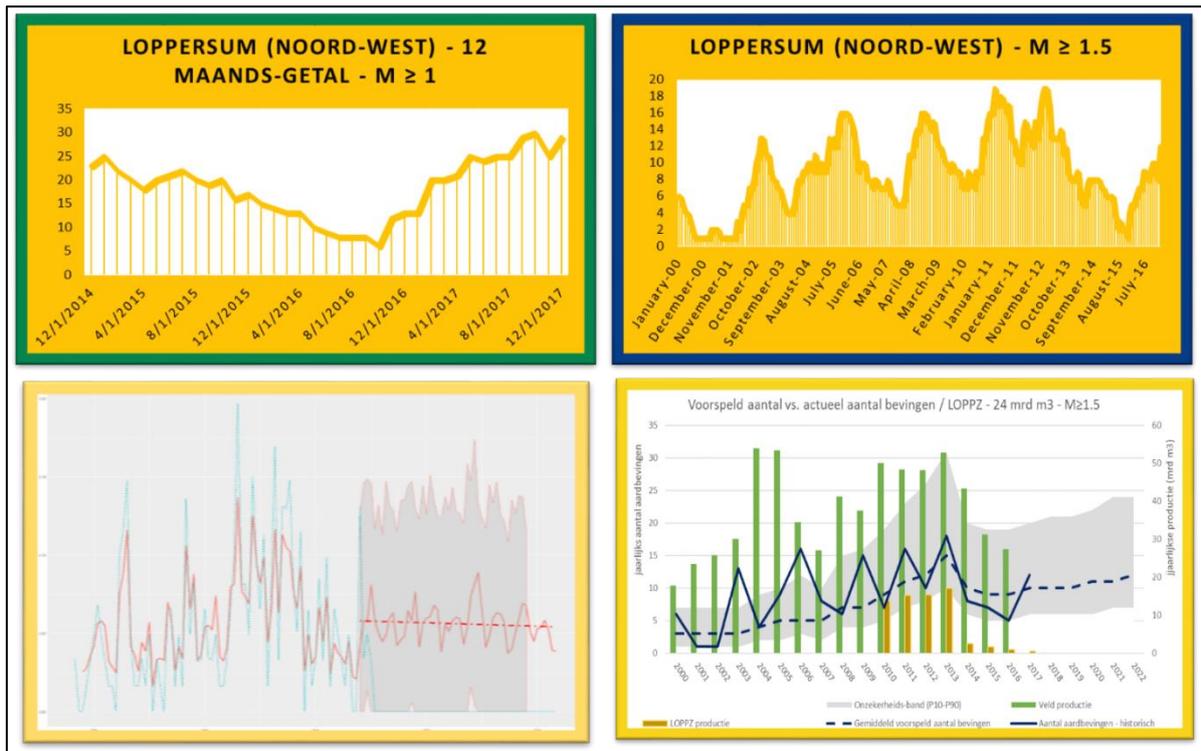
Figure 47   Loppersum observed trends (upper two panels) and forecasts (lower two panels). A full background to this figure is given in reference NAM, 2017g.

4.5.2   Probability earthquakes with higher magnitude and b-factor

The probability of higher magnitude earthquakes was reported in reference (NAM, 2017e) and is reproduced here for discussion purposes. It shows that the probability for having one or more earthquakes with a magnitude of 3.6 or higher is 16% for 2018. That probability increases to about 20% in 2022.

YEAR	M≥3.6	M≥4.0	M≥4.5	M≥5.0
2018	16.0%	6.6%	1.6%	0.4%
2019	17.0%	7.0%	1.6%	0.4%
2020	17.8%	7.5%	1.8%	0.4%
2021	19.3%	8.0%	1.9%	0.5%
2022	20.2%	8.7%	2.2%	0.6%

Table 5   Probability of higher magnitude earthquakes (reproduced from reference NAM, 2017e).

The so-called b-factor is only influenced by a small amount after the earthquake at Zeerijp (see Figure 48).
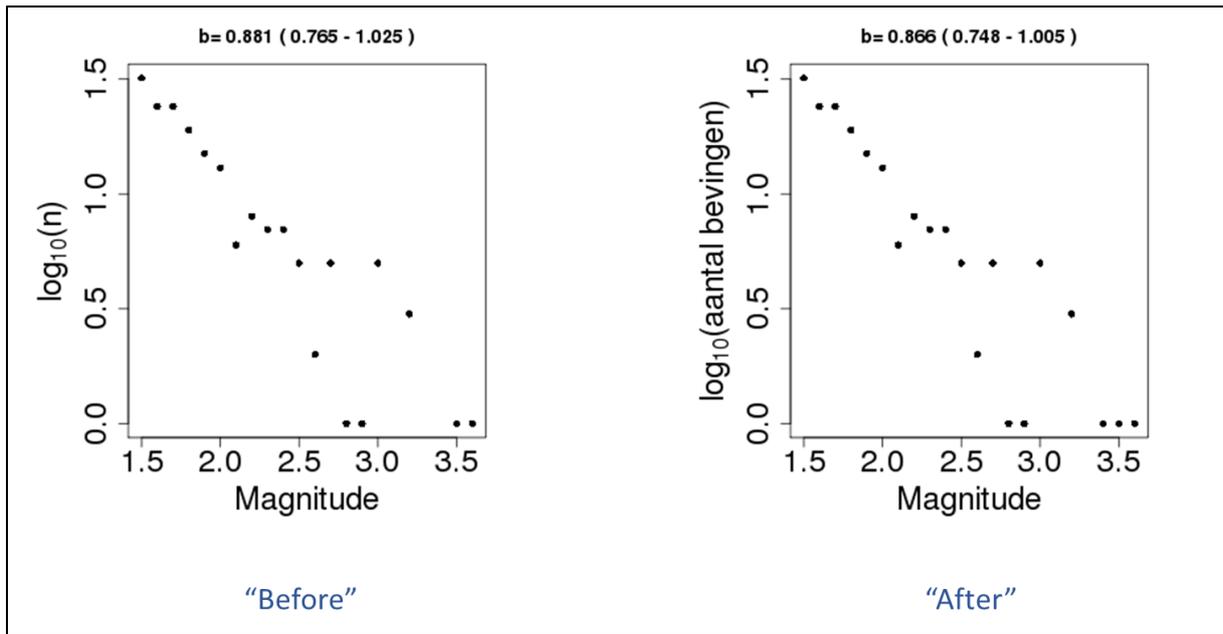
Figure 48   Estimates of the "b-factor", before and after the Zeerijp 3.4 earthquake.

5 Intervention measures and their estimated effect on seismicity

5.1 Qualitative coupling of intervention measures to the event

The PGA parameter of the MRP has been exceeded at the intervention level. In line with the MRP (see MRP, Figure 49) an assessment needed to be made which control measures (interventions) are required given the current circumstances. This assessment is done using a few contextual questions ("afwegingskader", see figure 49). NAM completed this assessment and advised SodM of these control measures in its letter of 10th January 10th (NAM, 2018a). As these measures included field-wide production-related measures that potentially affect other considerations (e.g. Security of Supply), the final decision is put to the Minister (ref. MRP, chapter 7, NAM 2017a).

As discussed in Chapter 4, the following considerations form the basis of the proposed potential control measures:

1. Apart from PGA, another parameter of the MRP (Earthquake density) also approached the intervention-level.
2. An ongoing upward trend in Loppersum earthquakes has been observed (despite producing only a minimum of volume from local clusters).
3. No anomalous PGA was observed (which means that GMPE is still valid).
4. The duration of the actual seismic event was short (less than 1 second), as expected.
5. The probability of such an event happening has been estimated at >16%, i.e. such an event is likely to happen approximately every 6 years.
6. The probability of having higher magnitude earthquakes has not materially changed after this event.
7. No DS2 damage caused by the earthquake has yet been observed.
8. No new area has become seismically active.
9. There are no special observations with respect to faults. (Note this will be studied further.)
10. The current increase in seismicity was predicted by our model (NAM, 2017e), occurred actually somewhat later than predicted.
11. The predicted number of earthquakes in Loppersum shows a stabilization/slow increase rather than a steep increase.

So, even though the event has been analyzed by NAM as significant in the context of the MRP, it is unlikely to lead to a new quantitative safety assessment (which would have made the event more significant).

Figure 49 (reproduced from NAM, 2017a, the MRP) shows the coupling of measures with exceedances of thresholds of MRP parameters.

Using Figure 49, it follows that control measures can range from "level 4" (prepare to close-in a cluster) to "level 10" (an immediate close-in of a large part of the Groningen production system). As argued in NAM's letter of 10th January (NAM, 2018a), closing-in of a group of clusters (LOPPZ) that is already producing a small amount of volume may not be sufficient to achieve a significant decline in yearly number of earthquakes. A "level-8" control measure, i.e. a volume reduction may need to be considered and, therefore, according to the MRP only the Minister can take the final decisions.
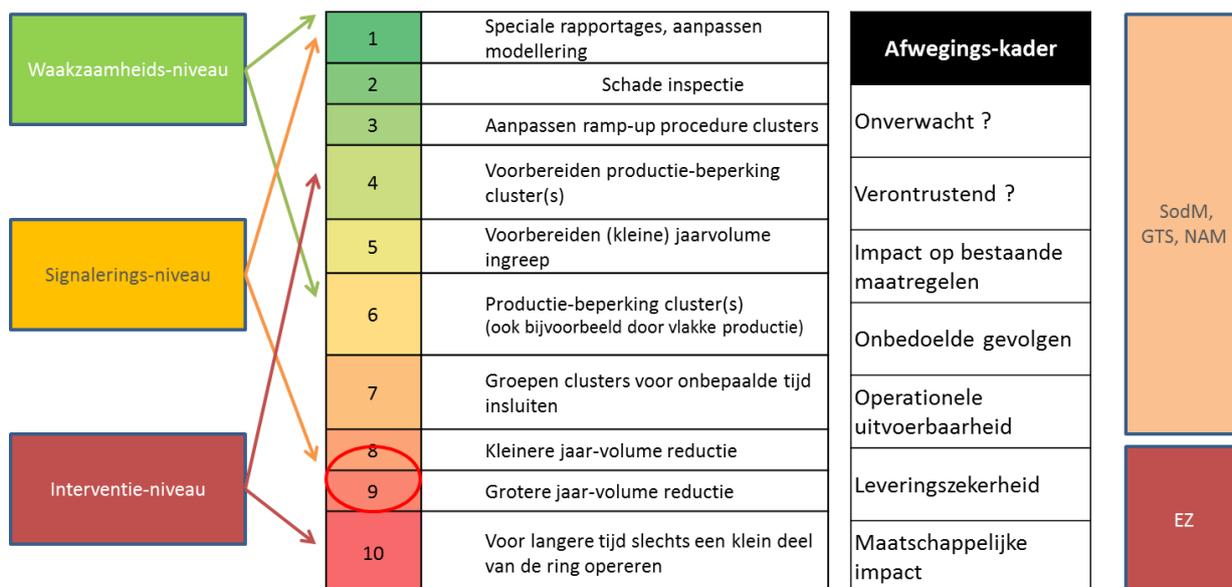
Figure 49 Coupling of production measures to the MRP threshold levels. For detailed description see (NAM, 2017a)

5.2 The estimated effect of control measures on seismicity

Table 6 shows a few first-order approximations estimating the potential effect control measures may have on the yearly number of earthquakes (M≥1.5).

Measure	Expected effect on yearly number of earthquakes (M≥1.5)	Basis
Volume reduction (new)	0.7 EQ per Bcm	Based on simulations with HRA model (NAM 2017e)
Volume reduction (2017, 10%, 2.4 Bcm)	Assumed that 50% of its effect not yet visible in EQ count – 0.8 EQ	Based on simulations with HRA model (NAM 2017e)
Closing in production clusters	3 LOPPZ clusters ~ 0.7 EQ – also effect on earth-quake density	Re-distribution study (NAM, 2017h)
	EKL ~ 0.7 EQ – no effect on earth-quake density	Re-distribution study (NAM, 2017h)
	Effect of close-in of remaining 2 clusters LOPPZ – assumed zero – treated as potential upside	Conservative estimate, based on re-distribution study (NAM, 2017h)
Effect of flatter production	Assumed zero; treated as potential upside	Conservative estimate

Table 6 Overview of estimates of effect of control measures on yearly number of earthquakes

The effect that a reduced number of earthquakes has on relevant MRP parameters is discussed in the next section. The approximations for estimating the effect of measures on the number of earthquakes are first order estimates in two ways:

1. Firstly, they are derived using insights from modelling work and statistics (its applicability is likely restricted to operating conditions of the field close to the current ones).
2. Secondly, because the natural variability of the parameters we are aiming to influence (nr of earthquakes, earthquake density) is large compared to the effect; to the extent that simply due to statistical variations the effect of reducing volume on the number of earthquakes may be even negative rather than positive, i.e. we may observe initially more earthquakes rather than less. This variability cannot be controlled, and is therefore a factor that must be taken into account when making decisions.

5.2.1 Volume reduction

The estimation of the effect of reducing volume on the number of predicted earthquakes is done using Figure 50. This figure has been derived from model runs of the Hazard and Risk model (NAM, 2017e). Volumes ranging from 24 Bcm to 0 Bcm were used as input and the resulting number of earthquakes (M≥1.5) were calculated. The effect on the number of earthquakes ranges from about 0.5/Bcm reduced to about 1/Bcm reduced depending on the year. The effect becomes, of course, somewhat bigger after a few years (of successively producing less). The approximation used to estimate the effect in the near to medium term is 0.7 EQ/Bcm.
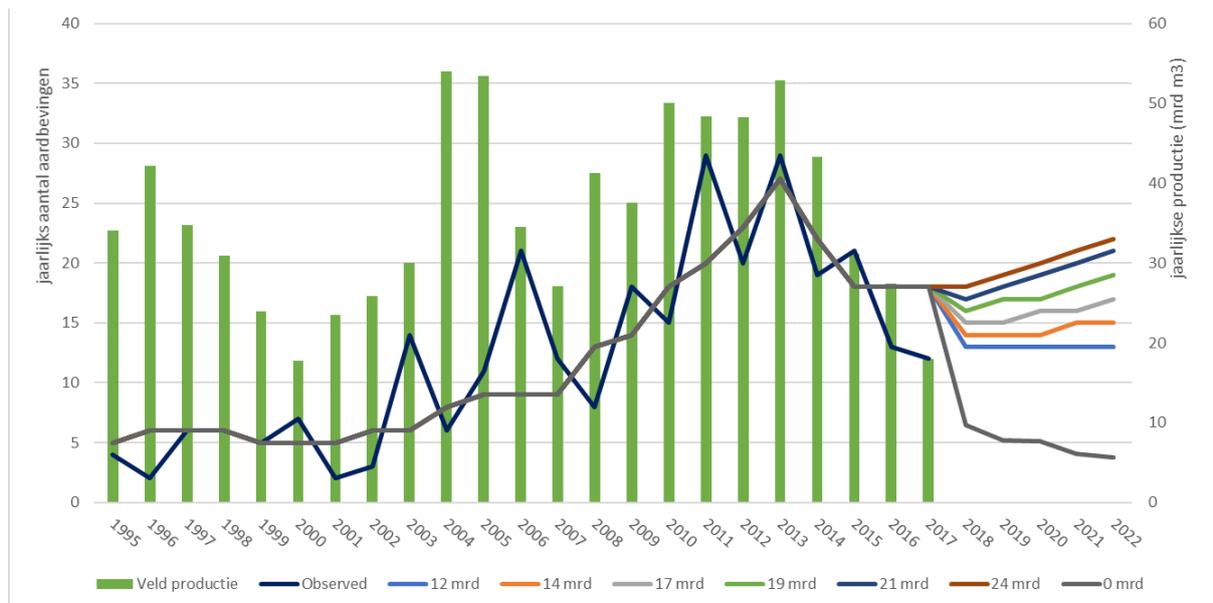
Figure 50   Predicted number of earthquakes for several production scenarios. Derived using the HRA model (NAM, 2017e).

5.2.2 Closing-in LOPPZ and EKL

The effect of closing in a (part of) the LOPPZ clusters and EKL was recently shown in NAM, 2017h. The results of that study have been summarized in a simple approximation of 0.7 earthquakes per year (M ≥ 1.5) associated with cessation of production in LOPPZ and the same for cessation of production in EKL.

5.2.3 Flatter production

Historically large swings in production characterized the Groningen field (due to fluctuations in gas demand), see Figure 51.
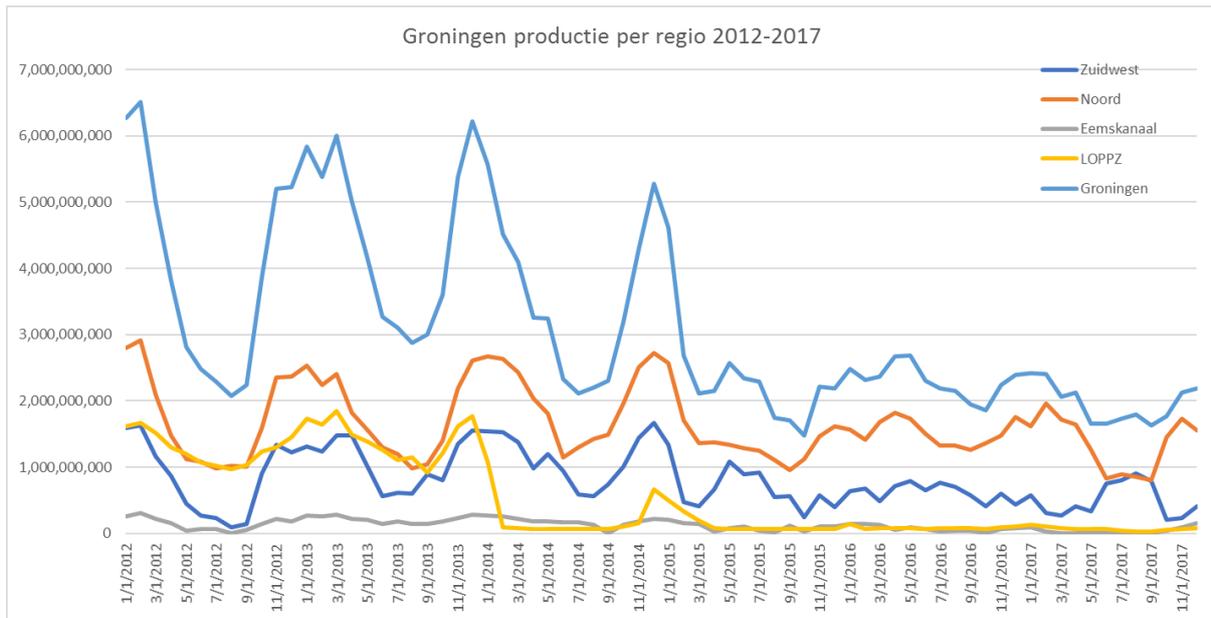
Figure 51   Groningen production per region showing the decrease of fluctuations over time since 2015.

However, more recently the production-swings have been much more dampened (see also Figure 51). Also, it has been difficult to quantify the positive effect of flatter production (although it is conceptually a reasonable effect to expect). So, at this moment, a conservative approach has been used and no "credit" in risk terms has been incorporated for implementing flatter production.   From a precautionary principle, flat production has been and will likely be implemented as much as other constraints allow.

5.2.4   Summing intervention measures

It is assumed that up to 30% volume reduction the benefit on seismicity of all the intervention measures may be summed as the control measures act essentially independently from each other. For volume reductions beyond 30% there is a linear decline (with field production level) of the effect of all measures except volume. This prevents over-estimation of benefit at higher levels of volume reduction.

5.3   Effect of a reduced yearly number of earthquakes on (MRP) parameters

After having made the assessment of the effect of potential intervention measures on the yearly number of earthquakes we now proceed to estimate the effect of a reduced number of earthquakes on the MRP parameters realizing that the underlying activity rate ultimately drives them.

The effect of reducing the number of earthquakes (M≥1.5) per year on MRP parameters is summarized in Table 7 below.

MRP parameter	Related to yearly number of earthquakes (M≥ 1.5)	Basis
Activity Rate	1:1	Trivial
Earth-quake density	0.015 point reduction per earthquake reduced	Statistical simulations
Yearly probability higher magnitude earthquake	1% reduction (absolute) in probability per earthquake less (conservative value for Loppersum area)	Statistical calculation using the Groningen Gutenberg-Richter relations

Table 7. Linking a reduced number of earthquakes to key MRP parameters

The basis for this table is provided in the following subsections.

5.3.1 The effect on earthquake density

Earthquake density, as an MRP parameter, was introduced to monitor possible early indications that seismicity in an area is increasing, with an indication for a possible higher magnitude earthquake in that area. In addition, the parameter can be used as a proxy for "nuisance".

Earthquake density is calculated parameter and is driven by the (yearly) number of earthquakes. To estimate the effect of a reduction in number of earthquakes on earthquake density, a simple approach would be to use proportionality, i.e. a decrease of say 30% in yearly number of earthquakes would lead to a 30% decrease in earthquake density. This proportionality, however, is likely to be an overestimate of the effect, as suggested by both simulations and historic data.

Based on the method introduced in the Special Report Loppersum earthquakes (NAM, 2017g), simulations were made to calculate the effect of a reducing number of earthquakes on earthquake density. Figure 52 shows the results of simulation of earthquake density as function of underlying (reduced) number of M≥1 earthquakes.
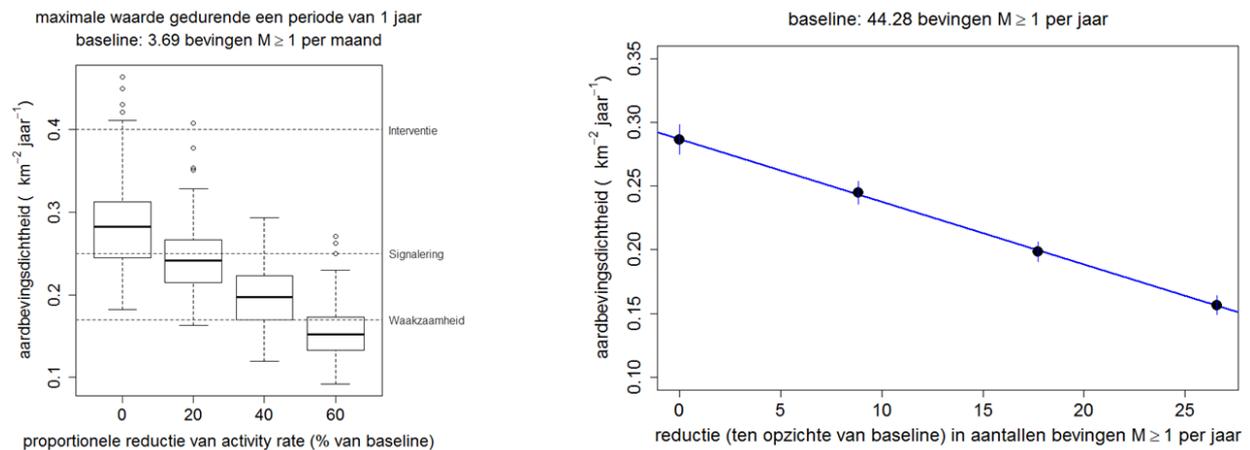
Figure 52   Simulated effect of reducing number of earthquakes on the earthquake density

The left-hand panel shows the reduction in earthquake density as a function of the % reduction in activity rate (M≥1). The black bold lines in the box-and-whiskers shows the average expected earthquake density. The whiskers show the (simulated uncertainty). The right-hand graph shows earthquake density as a function of reduction in number of earthquakes. The relationship is linear and the slope of the graph is used to derive the approximation for earthquake density reduction as a function of number of earthquakes (in turn as a function of reducing volume).

5.3.2 Effect on the probability of higher-magnitude earthquakes

The last parameter considered is strictly speaking not an MRP parameter but probably interesting nevertheless. The (yearly) number of earthquakes does not only drive the calculated earthquake density but is also likely to drive the probability of a higher-magnitude earthquake. In the Groningen field, a distinction can be made between the area around Loppersum where the probability of having a higher magnitude earthquake is somewhat more sensitive to the number of "small earthquakes" (a lower "b-factor", Gutenberg-Richter) than the rest of the Groningen field.

The estimated effect of the yearly number of earthquakes on the probability of higher-magnitude earthquake is shown in 2 tables, one for Loppersum, one for the rest of the field.

Yearly number M≥1.5 earth-quakes	Probability (%) - Loppersum	Yearly number M≥1.5 earth-quakes	Probability (%) – rest Groningen field
3	5	3	0.8
10	14	10	2.7
13	18	13	3.5
15	21	15	4.1
16	22	16	4.3
17	23	17	4.6
18	24	18	4.9
19	25	19	5.1

Table 8   Probability (%) of having at least 1 earthquake with a magnitude of M≥3.6 for this yearly number of earthquakes (M≥1.5, column left) in the Loppersum area (yellow table left, b-value=0.9) and for the rest of the field (blue table, b-value = 1.1).

It is clear from these tables that a reduction in number of earthquakes of M≥1.5 is expected to have a much more profound effect on the probability of higher magnitude earthquakes in the Loppersum area than in the rest of the Groningen field (i.e. a production reduction is more effective in reducing that probability). The approximation of, about 1% reduction in probability of a higher magnitude earthquake per 1 earthquake (M≥1.5), is derived from Table 9Table 8.

Aantal bevingen elders in het Groningen gasveld
(buiten Loppersum en omstreken)

	3	4	5	6	7	8	9	10	11	12	13	14	15	16	17	18	19
3	5.3	5.5	5.8	6.1	6.3	6.6	6.8	7.1	7.4	7.6	7.9	8.1	8.4	8.6	8.9	9.1	9.4
4	6.7	7.0	7.2	7.5	7.7	8.0	8.3	8.5	8.8	9.0	9.3	9.5	9.8	10.0	10.3	10.5	10.8
5	8.1	8.4	8.6	8.9	9.1	9.4	9.6	9.9	10.1	10.4	10.6	10.9	11.1	11.4	11.6	11.9	12.1
6	9.5	9.8	10.0	10.3	10.5	10.8	11.0	11.3	11.5	11.8	12.0	12.2	12.5	12.7	13.0	13.2	13.5
7	10.9	11.1	11.4	11.6	11.9	12.1	12.4	12.6	12.9	13.1	13.3	13.6	13.8	14.1	14.3	14.5	14.8
8	12.3	12.5	12.7	13	13.2	13.5	13.7	13.9	14.2	14.4	14.7	14.9	15.1	15.4	15.6	15.8	16.1
9	13.6	13.8	14.1	14.3	14.5	14.8	15.0	15.2	15.5	15.7	15.9	16.2	16.4	16.6	16.9	17.1	17.3
10	14.9	15.1	15.4	15.6	15.8	16.1	16.3	16.5	16.8	17.0	17.2	17.5	17.7	17.9	18.1	18.4	18.6
11	16.2	16.4	16.7	16.9	17.1	17.3	17.6	17.8	18.0	18.3	18.5	18.7	18.9	19.2	19.4	19.6	19.8
12	17.5	17.7	17.9	18.1	18.4	18.6	18.8	19.0	19.3	19.5	19.7	19.9	20.2	20.4	20.6	20.8	21.0
13	18.7	18.9	19.2	19.4	19.6	19.8	20.1	20.3	20.5	20.7	20.9	21.2	21.4	21.6	21.8	22.0	22.2
14	20.0	20.2	20.4	20.6	20.8	21.1	21.3	21.5	21.7	21.9	22.1	22.4	22.6	22.8	23.0	23.2	23.4
15	21.2	21.4	21.6	21.8	22.0	22.3	22.5	22.7	22.9	23.1	23.3	23.5	23.7	24.0	24.2	24.4	24.6
16	22.4	22.6	22.8	23.0	23.2	23.4	23.6	23.9	24.1	24.3	24.5	24.7	24.9	25.1	25.3	25.5	25.7
17	23.5	23.8	24.0	24.2	24.4	24.6	24.8	25.0	25.2	25.4	25.6	25.8	26.0	26.2	26.5	26.7	26.9
18	24.7	24.9	25.1	25.3	25.5	25.7	25.9	26.2	26.4	26.6	26.8	27.0	27.2	27.4	27.6	27.8	28.0
19	25.8	26.1	26.3	26.5	26.7	26.9	27.1	27.3	27.5	27.7	27.9	28.1	28.3	28.5	28.7	28.9	29.1

(Aantal bevingen in het gebied Loppersum en omstreken — left axis)

Table 9   The probability of having on 1 or more earthquake (M≥3.6) in the Groningen gas-field given 2 parameters; 1) the number of earthquakes in the Loppersum area, and 2) the number of earthquakes in the rest of the field

5.3.3 Summary table of (volume) effect

Finally, using all approximations discussed above a table can compiled that relates reductions in Groningen volume (in combination with the other aforementioned measures of Table 6 and Table 7) to anticipated reduction in (MRP) parameters (Table 10).

Groningen Jaarvolume (bln Nm3)	% volume reduced	Activity Rate (jaar $^{-1}$)	Probability Earth-quake M ≥ 3.6	Earth-quake density (proportional) (km^{-2} jaar^{-1})	Earth-quake density (simulated) (km^{-2} jaar^{-1})
21.6	0%	18	16%	0.38	0.38
19.4	10%	14	12%	0.28	0.34
17.3	20%	13	11%	0.25	0.31
15.1	30%	11	9%	0.22	0.29
13.0	40%	10	8%	0.20	0.27
10.8	50%	9	7%	0.17	0.25
8.6	60%	8	6%	0.15	0.24
6.5	70%	6	5%	0.12	0.22
4.3	80%	5	4%	0.10	0.20
2.2	90%	4	3%	0.07	0.18
0.0	100%	3	2%	0.05	0.16

Table 10   The anticipated effect of volume reductions on a few MRP parameters using approximations derived from modeling and statistics

The apparent non-linearity of the first row in the table is because for the first 10% volume reduction, all other measures (close-in LOPPZ etc.), are assumed to be introduced as well. The second notable feature in this table occurs when volume reductions beyond 30% are considered because beyond 30% independence of effects is no longer assumed (see above).

As discussed in the sections above, the table is a first-order approximation, based on our main model (NAM, 2017e), and is associated with caveats:

- Our models are adequately calibrated, yet are only models nevertheless and as such can only be expected to yield an approximation of reality.
- The variability in the range of expected outcomes is typically larger than the level of control that can be applied by the various system levers (e.g. redistribution of production, reducing total offtake).
- The applicability of the rules is only valid for certain time-periods, in a the specific (recent) context,
- The effects of the interventions are likely temporary (in our modeling view) and effects are likely to disappear over time (~10 year)

That said, these results provide a reasonable assessment of the effects that can be expected of the potential control measures that NAM advised in its letter of 10th January.

6 References

1. Bommer, J.J., B. Dost, B. Edwards, P.J. Stafford, J. van Elk, D. Doornhof & M. Ntinalexis (2016). Developing an application-specific ground-motion model for induced seismicity. Bulletin of the Seismological Society of America 106(1), 158-173.

2. Bommer, J.J., P.J. Stafford, B. Edwards, B. Dost, E. van Dedem, A. Rodriguez-Marek, P. Kruiver, J. van Elk, D. Doornhof & M. Ntinalexis (2017a). Framework for a ground-motion model for induced seismic hazard and risk analysis in the Groningen gas field, The Netherlands. Earthquake Spectra 33(2), 481-498.

3. Bommer, J.J., B. Edwards, P.P. Kruiver, A. Rodriguez-Marek, P.J. Stafford, B. Dost, M. Ntinalexis, E. Ruigrok & J. Spetzler (2017b). V5 Ground-Motion Model for the Groningen Field. 30 October, 161 pp. Available for free download from link at foot of page.

4. Bommer, J.J., P.J. Stafford and M. Ntinalexis, Empirical Ground-Motion Prediction Equations for Peak Ground Velocity from Small-Magnitude Earthquakes in the Groningen Field Using Multiple Definitions of the Horizontal Component of Motion - Updated Model for Application to Smaller Earthquakes, , November 2017, 2017c

5. Bommer, J.J., B. Edwards, P.P. Kruiver, A. Rodriguez-Marek, P.J. Stafford, B. Dost, M. Ntinalexis, E. Ruigrok, J. Spetzler, V5 Ground-Motion Model for the Groningen Field, 30th October 2017, 2017d.

6. Bommer, J.J., B. Dost, B. Edwards, P.P. Kruiver, M. Ntinalexis, A. Rodriguez-Marek, P.J. Stafford & J. van Elk (2018). Developing a model for the prediction of ground motions due to earthquakes in the Groningen gas field. Netherlands Journal of Geoscience, in press.

7. Crowley, H., B. Polidoro, R. Pinho & J. van Elk (2017). Framework for developing fragility and consequence models for local personal risk. Earthquake Spectra 33(4), 1325-1345, 2017.

8. Dost, B., E. Ruigrok & J. Spetzler (2018). Development of probabilistic seismic hazard assessment for the Groningen gas field. Netherlands Journal of Geoscience, in press.

9. Kruiver, P. P., E. van Dedem, E. Romijn, G. de Lange, M. Korff, J. Stafleu, J.L. Gunnink., A. Rodriguez-Marek, J.J. Bommer, J. van Elk & D. Doornhof (2017). An integrated shear-wave velocity model for the Groningen gas field, The Netherlands. Bulletin of Earthquake Engineering 15(9), 3555-3580.

10. NAM (Jan van Elk and Dirk Doornhof, eds), Technical Addendum to the Winningsplan Groningen 2016 - Production, Subsidence, Induced Earthquakes and Seismic Hazard and Risk Assessment in the Groningen Field, PART V - Damage and Appendices, Nederlandse Aardolie Maatschappij BV 1st April 2016, 2016a.

11. NAM, Meet- en Regelprotocol Groningen veld, June 2017a.

12. NAM, Rapportage Seismiciteit Groningen - 1 november 2017, November 2017b.

13. NAM, Trillingsschade aan gebouwen, Informatiedocument – versie 1.0, NAM, June 2017, 2017c.

14. NAM, Van Oeveren, Henk, Valvatne, Per and Geurtsen, Leendert, Groningen Dynamic Model Updates 2017, Assen : NAM, 2017. EP201708205454, 2017d

15. NAM, J. van Elk and D. Doornhof, Hazard, Building Damage and Risk Assessment for the Groningen Area, November 2017, 2017e.

16. NAM, Rapportage Seismiciteit Groningen - 1 November 2017, 2017f

17. NAM, Special Report on the Loppersum Earthquakes, December 2017, 2017g

18. NAM, Geurtsen, Leendert and Valvatne, Optimisation of the Production Distribution over the Groningen field to reduce Seismicity, 2017h

19. NAM, Evaluatie en aanbevelingen voorbeheersmaatregelen: Zeerijp aardbeving, Letter 19-1-2018, Brief Ref.:EP201801201646, 2018a

20. NAM, Zeerijp beving beheersmaatregelen, Letter 17-1-2018, Brief Ref. EP201801203705, 2018b

21. Noorlandt, R.P., P.P. Kruiver, M.P.E. de Kleine, M. Karaoulis, G. de Lange, A. Di Matteo, J. von Ketelhodt, E. Ruigrok, B. Edwards, A. Rodriguez-Marek, J.J. Bommer, J. van Elk & D. Doornhof (2018). Characterisation of ground-motion recording stations in the Groningen gas field. Journal of Seismology DOI: 10.1007/s10950-017-9725-6.

22. TNO-034-DTM-2009-04435, Kalibratiestudie schade door aardbevingen, 11 November 2009

23. USGS, "Did you feel is?" Internet micro-seismic intensity maps, Wald, Quitoriano, Worden, Hopper and Dewey, Annals of Geophysics 54, 6, 2011.

The NAM reports can be downloaded from:

https://www.nam.nl/feiten-en-cijfers/onderzoeksrapporten.html#